

Development & Characterization of High Entropy Stabilized Bond Coat for Gas Turbine Blade Applications



By

Kashif Mehmood

School of Chemical and Materials Engineering

National University of Sciences and Technology

2021

Development & Characterization of High Entropy Stabilized Bond Coat for Gas Turbine Blade Applications



Name: Kashif Mehmood

Reg. No: NUST2017 MSE12-00000206118

**This thesis is submitted as a partial fulfillment of the requirements
for the degree of**

MS in (Materials and Surface Engineering)

Supervisor Name: Dr. Malik Adeel Umer

School of Chemical and Materials Engineering (SCME)

National University of Sciences and Technology (NUST)

H-12 Islamabad, Pakistan

August, 2021



C7EE ✓

National University of Sciences & Technology (NUST)

MASTER'S THESIS WORK

Formulation of Guidance and Examination Committee (GEC)

Name: Kashif Mehmood
 Department: Materials Engineering
 Credit Hour Completed: 24

NUST Regn No: 00000206118
 Specialization: Mat & Surface Engineering
 CGPA: 3.13

Course Work Completed

S/No	Code	Title	Core/Elective	CH	Grade
1	MSE-822	Fractography & failure Analysis	Elective	03	B+
2	MSE-811	Material Thermodynamics	Core	03	C+
3	MSE-821	Mechanical Behavior of Materials	Core	03	B
4	MSE-812	Phase Transformation & Microstructures	Core	03	B
5	MSE-851	Surface Engineering & Characterization	Core	03	B
6	MSE-872	Composite Materials	Elective	03	B+
7	MSE-854	Characterization of Materials	Elective	03	B
8	MSE-871	Polymer Engineering	Elective	03	B+
9	MSE-898	Research Methodology	Additional	02	Q

Date: Feb 2019

Student's Signature

Thesis Committee

1. Name: Dr. Malik Adeel Umar (Supervisor)
 Department: SCME, Materials Engineering

Signature:

2. Name: Dr. Zuhair S Khan (GEC Member)
 Department: USPCAS-E

Signature:

3. Name: Dr. Ahmed Umar Munawar (GEC Member)
 Department: SCME, Materials Engineering

Signature:

4. Name: _____
 Department: _____

Signature: _____

Date: 23/4/19

Signature of Head of Department:

APPROVAL

Date: _____

23/4/19
Dean/Principal**Distribution**

- 1x copy to Exam Branch, Main Office NUST
 1x copy to PGP Dte, Main Office NUST
 1x copy to Exam branch, respective institute

School of Chemical and Materials Engineering (SCME) Sector H-12, Islamabad

National University of Sciences & Technology (NUST)
 MASTER'S THESIS WORK
 PETITION FOR CHANGE IN THE GUIDANCE COMMITTEE

Date: 14/10/20

Name: Kashif Mehmood
 Department: Materials Engineering

Regn No: 00000206118
 Specialization: MS (Materials & Surface Engineering)

COMMITTEE MEMBERS CHANGES

(Signatures of those to be deleted are required, if signature for deletion cannot be obtained, type the reason on the signature line)

Delete
 Signature: (Left NUST)
 Name: Dr. Ahmed Umair Murawar
 Department: _____

Add
 Signature: _____
 Name: Dr. Muhammad Shahid
 Department: Materials Engineering

Delete
 Signature: _____
 Name: _____
 Department: _____

Add
 Signature: _____
 Name: Dr. Mohsin Saleem
 Department: Materials Engineering

SUPERVISOR/CO-SUPERVISOR CHANGES

(Signatures of those to be deleted are required, if signature for deletion cannot be obtained, type the reason on the signature line)

Delete
 Signature: _____
 Name: _____
 Department: _____

Add
 Signature: _____
 Name: _____
 Department: _____

Signature of Supervisor (Dr. Adeel Umair)

Signature of Head of Department

Signature of Student

Date 14/10/20

APPROVED15-1-2021

Date

Signature of Dean/Principal



National University of Sciences & Technology (NUST)

FORM TH-4

MASTER'S THESIS WORK

We hereby recommend that the dissertation prepared under our supervision by

Regn No & Name: 00000206118 Kashif Mehmood

Title: Development & Characterization of High Entropy Stabilized Bond Coat for Gas Turbine Blade Applications.

Presented on: 13-08-2021 at: 1500 hrs in SCME Seminar Hall

Be accepted in partial fulfillment of the requirements for the award of Masters of Science degree in Materials & Surface Engineering.

Guidance & Examination Committee Members

Name: Dr Zuhair S Khan

Signature: ZS Khan

Name: Dr Mohsin Saleem

Signature: Mohsin Saleem

Name: Dr Muhammad Shahid

Signature: Muhammad Shahid 17/8/21

Supervisor's Name: Dr Malik Adeel Umar

Signature: Malik Adeel Umar

Dated: 20-8-21

[Signature]

Head of Department

Date 25/8/2021

[Signature]

Dean/Principal

Date 25.8.2021

DEDICATION

*I dedicate this thesis to my loving and caring
Mother, my beloved father, my brothers and
my sister.*

Acknowledgments

All admiration to Allah Almighty who is all omnipotent and Regulator of the whole Universe. He is the only One, who bestows and gives the power to us to think, utilize our expertise in knowledge in achieving remarkable solutions for mankind in every field. Therefore, I express my greatest obligations to Almighty Allah the universal and the architect of all universe, who has gifted us a brain, intelligence and unhinged nature creation of knowledge and physique to achieve our desired work in the form of this project report. As Almighty Allah Almighty says in Quran:

“Read! In the name of your Lord” (Alaq; 1st revealed ayah)

This Quranic verse sums up the entire importance of education in the lives of humans.

I would like to express my gratefulness to my very nice and respected supervisor Dr. Malik Adeel Umer for their clear and patient guidance that directed me to fulfill my research project and this thesis. Their cool and calm behavior motivated me to do my best. Also, I am very grateful to Dr. Ahmed Umar Munawar who helped me and motivated me to do my best. Their valuable suggestions and feedback contributed to this thesis. I would also express thanks to Mr. Tanveer Hussain Shakar who guided and motivated me like big brother and also my parents, family members and my friends especially Mr. Muhammad Imran who helped me and stayed with me in this period, their prayers, support and valuable suggestions.

I acknowledge the support provided by the Materials Engineering department of SCME, Aerospace Center (DLR) Germany & Bartin University, Turkey for providing me a platform to perform my experiments and using my skills in research work.

I acknowledge the dedication and help of Mr. Muhammad Ilyas Safi, during my research. Last, but not the least, I want to thank my family for their prayers, support and confidence on me without which I would not have been able to reach my full potential.

Kashif Mehmood

Abstract

Thermal Barrier Coating (TBC) are an integral part of present-day gas turbines for both power generation and aerospace applications. TBCs consist of a top coat (ceramic) and a bond coat which are deposited on top of a superalloy substrate to withstand high temperatures, corrosion, oxidation and stress conditions. During the high temperature exposure, an oxide layer starts to grow between the bond coat & the ceramic top coat which is called as thermally grown oxide (TGO). Composition and morphology of TGO plays a very vital role in improving the lifetime of a TBC system, and is dependent on the bond coat composition. In this study, high entropy stabilized bond coat will be deposited and tested for the bond coat in a TBC system. High entropy materials are one of the latest developed material systems which consist of 4 or more elements present in equi-atomic compositions. High configurational entropy of these materials helps them to achieve greater stability at elevated temperatures. In addition, these materials show sluggish diffusion effect which is beneficial in bond coats to reduce the diffusion of different elements from the metallic superalloy substrate to the TGO.

In the present study, high entropy- based bond coat will be developed by adding Ni, Co, Cr, Fe and Al in near equi-atomic compositions. Effect of process parameters along with post-deposition annealing on the microstructure of bond coats and the resulting thermally grown oxide will be investigated. In addition, some minor additions of refractory elements could be made to further tailor the TGO composition to achieve longer lifetime of TBC systems. The testing of TBC systems will be carried out at temperature of around 1000°C. Gas turbines used for power generation applications usually experience such isothermal conditions where the TBC systems deposited on the gas turbine blades have to withstand such high temperatures for longer period of time. The TBC system deposited in this study will be characterized in the as-coated condition and after testing at 1000°C for 5, 15, 50 and 100hrs.

Table of Contents

CHAPTER 1	INTRODUCTION	1
1.1	OVERVIEW OF THERMAL BARRIER COATINGS	1
1.1.1	Super-alloy Substrate	2
1.1.2	Bond Coat (BC)	3
1.1.3	Thermally Grown Oxide (TGO)	3
1.1.4	Top Coat (TC).....	4
1.2	APPLICATIONS OF THERMAL BARRIER COATINGS.....	4
1.3	HIGH ENTROPY ALLOYS	5
1.4	THERMAL SPRAYING.....	5
1.4.1	Atmospheric Plasma Spraying	6
1.4.2	High Velocity Oxy-Fuel Spraying (HVOF)	8
1.4.3	Flame Spraying	9
CHAPTER 2	LITERATURE REVIEW.....	10
CHAPTER 3	EXPERIMENTATION METHODS	18
3.1	BALL MILLING (MIXING) OF ELEMENTAL POWDERS	18
3.1.1	Merits	19
3.1.2	Demerits:	19
3.2	SAMPLES PREPARATION FOR COATINGS	19
3.2.1	Pre Surface Treatment.....	20

3.2.2	Grit Blasting.....	20
3.2.3	Pre-heating of Substrates and Powder	21
3.3	ATMOSPHERIC PLASMA SPRAYING COATING OF SAMPLES.....	21
3.3.1	Merits:.....	22
3.3.2	Demerits:.....	23
3.4	ANNEALING OF COATINGS	23
3.4.1	Aims and Objective.....	23
CHAPTER 4 CHARACTERIZATION TECHNIQUES.....		24
4.1	SCANNING ELECTRON MICROSCOPE (SEM):	24
4.2	X-RAY DIFFRACTION (XRD).....	25
4.3	HARDNESS TESTING OF COATINGS.....	26
4.4	ROUGHNESS TESTING.....	27
CHAPTER 5 RESULTS AND DISCUSSIONS.....		28
5.1	XRD ANALYSIS FOR PHASE IDENTIFICATION.....	28
5.2	AS-COATED HIGH ENTROPY COATINGS.....	28
5.3	AS-ANNEALED HIGH ENTROPY COATINGS	29
5.4	AFTER ISOTHERMAL OXIDATION TESTING.....	31
5.5	SEM ANALYSIS OF COATINGS (MICROSTRUCTURE STUDIES).....	32
5.5.1	SEM analysis in as-coated condition	32
5.5.2	SEM analysis in as-annealed condition	33

5.6 SEM ANALYSIS AFTER OXIDATION TESTING OF COATINGS	35
5.7 MICRO VICKERS HARDNESS	36
5.8 ROUGHNESS TESTING.....	36
5.9 POTENTIODYNAMIC/CORROSION BEHAVIOR TESTING	38
CHAPTER 6 CONCLUSION AND FUTURE WORK	42
6.1 CONCLUSION.....	42
6.2 FUTURE WORK.....	43
CHAPTER 7 REFERENCES	44

List of Figures

Figure 1. Anatomy of Thermal Barrier Coating	2
Figure 2. Schematics of Thermal Spraying.....	6
Figure 3. Principle of Plasma Spraying	6
Figure 4. Schematic of a Plasma Spraying System.....	7
Figure 5. Principle of High Velocity Oxy-Fuel Spraying.....	8
Figure 6. Components of a HVOF Spraying System.....	9
Figure 7. Ball Milling (2-Roll) apparatus at SCME.....	19
Figure 8. Atmospheric Plasma Spraying System: 9MC Controller & 9MB Nozzle .	21
Figure 9. Tube Furnace at Heat Treatment Lab SCME (NUST)	23
Figure 10. (a) JOEL JSM-6490LA SEM at SCME; (b) Schematics of SEM.....	25
Figure 11. XRD present at SCME- NUST (b) XRD basic schematics.....	26
Figure 12. Micro Hardness Testing equipment at SCME.....	27
Figure 13. SE700 Roughness Tester	27
Figure 14. XRD analysis of the coatings in as-coated condition	29
Figure 15. XRD analysis after annealing of coatings	30
Figure 16. X-ray diffraction results after Oxidation Testing	31
Figure 17. SEM micrographs of Coatings in as-Coated condition with varied Stand-off distances	32
Figure 18. Enlarged view of the as-coated Microstructure	33

Figure 19. Microstructure of Annealed Coatings at 1000°C for 4hrs.....	34
Figure 20. SEM images after Isothermal Oxidation Testing of Coatings.....	35
Figure 21. Micro Hardness Values of SS 316L, APS Coating and Annealed Coating	37
Figure 22. Surface Roughness	38
Figure 23. Samples after Potentiodynamic Testing in 3.5% NaCl solution	39
Figure 24. Curves depicting Potentiodynamic polarization/Corrosion performance of SS 316L, Coated & Annealed Sample in 3.5% NaCl	40

List of Tables

Table 1. Parameters for Grit blasting	20
Table 2. Plasma Spraying Operating Parameters	22
Table 3. Hardness Measurement Values	36
Table 4. Roughness measurements of coatings	37
Table 5. Electrochemical data of Stainless Steel 316L, Coated Sample and Annealed Sample acquired after Corrosion Behaviour Testing in 3.5% NaCl solution	41

List of Abbreviations

HEA	High Entropy Alloy
TBCs	Thermal Barrier Coatings
APS	Atmospheric Plasma Spraying
b.c.c	body center cubic
f.c.c	face center cubic
BC	Bond Coat
BSE	Backscattered electrons
EDX	Energy Dispersive X-ray
Fe	Iron
HVOF	High Velocity Oxy-Fuel
Ni	Nickel
O	Oxygen
SE	Secondary electrons
SEM	Scanning Electron Microscopy
Cr	Chromium
wt%	weight percent
at%	atomic percent
XRD	X-ray diffraction
JCPDS	Joint Committee on Powder Diffraction Standard

Chapter 1

Introduction

Conventional or known alloys are founded on basis of one primary element. Small amounts of diverse alloying elements are then added to the major element to mend its properties which forms alloy or an alloy series based on the principal element, thus it could produce limited alloys. For this purpose the alloying of multi-elements was first introduced by Yeh et al. in 1996 and reported in his publication in 2004[1] and coined as High Entropy Alloys (HEAs). Later on Cantor et al. named them as ‘multi-component alloys’ in the same year[2].

Continuous development of gas turbine engines is aided by efforts in various areas of science and engineering. These include designs of the efficient and modern turbines, better understanding, utilization and optimization of the combustion processes. In this regard endless efforts are being made to increase the efficiency of these turbine engines. Development of materials & manufacturing technology in this context is divided in three sub categories: (i) alloy substrate development to sustain more high temperature and better corrosion resistance; (ii) improvements in manufacturing technology to produce single crystal blades for improved creep resistance and intricate channels for cooling purpose and better heat transfer;(iii) application of the bond coat & top coat of ceramic on super alloy components for thermal insulation. There is a significant increase in insistence for this type of engineering coatings as compared to past decade. Eco-friendly aspects, harsh environments and extreme temperatures are always considered as a vital part of the designing while formulating the process[3]. For having lower environmental impact and economic effectiveness we must hence pay devotion to processes that use the least resources. The coatings applied upon the superalloy for increasing its life and the efficiency of turbine blades and engine are called as Thermal Barrier Coatings (TBCs).

1.1 Overview of Thermal Barrier Coatings

Thermal Barrier Coatings (TBCs) are being used to protect metallic components, as in gas-turbine engines, both land based and in aero applications for their protection against the hot burner gases which lead to surge in operating temperatures and thus the efficacy of turbine engines[4]. Augmented thermal efficiency stresses for the

innovative gas turbine engines edict that operating temperature must be increased significantly[5, 6]. This should be achieved without the structural or any physical failure of the components resulting from melting, thermal fatigue, oxidation, creep or some other damage mechanisms thus, the temperature at exposed surface of these integrant must be retained low enough to preserve properties of material within the tolerable boundary conditions.

Thermal Barrier Coatings (TBCs) have a complex metallic-ceramic structure (100 to 600 μm thick) which is specially designed to provide thermal and oxidation protection in gas turbine engines operating at elevated temperatures[7]. A thermal barrier coating system contains 4 layers in which two are metallic while other two are of ceramic nature as shown in Figure 1. These layers from innermost to outermost are: (1) the super-alloy substrate, designed to sustain mechanical loads, (2) the bond coat (BC) which provides oxidation resistance, (3) TGO(thermally grown oxide) resulted due to bond coat oxidation & (4) the ceramic top coat (TC) for protection against thermal loads and extreme environments[5, 8].

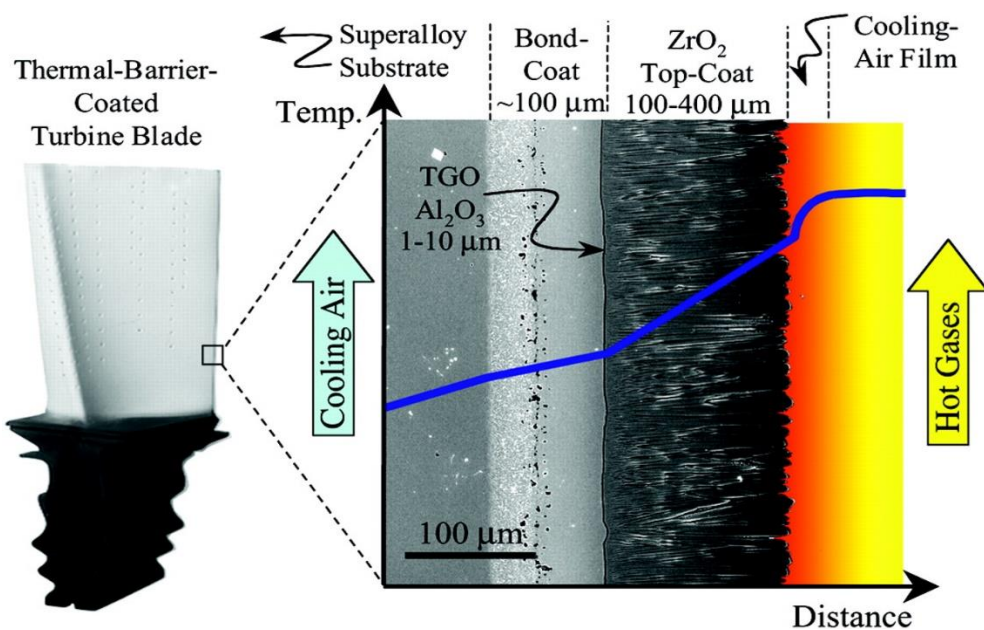


Figure 1. Anatomy of Thermal Barrier Coating

1.1.1 Super-alloy Substrate

Substrate material is always nickel or cobalt-based structural superalloy, designed to sustain mechanical loads which is internally air-cooled via inner hollow channels,

therefore forming a temperature descent across the module wall [9-11]. The superalloy section is an investment-casting in a polycrystalline or single-crystal form, and it may contain 5 to 12 supplementary elements which are added for the augmentation of particular properties such as strength at high-temperature[12], ductility[13], oxidation resistance[6], resistance to hot-corrosion[14], & cast ability. At elevated temperatures during process in gas-turbine engines, diffusion of different elements of high relative concentration value may occur b/w the superalloy substrate and the bond-coat[15].

1.1.2 Bond Coat (BC)

A bond-coat is a metallic layer which is resistant to oxidation and is usually 75 ~150 μm in its thickness[16]. The main purpose of the bond coat is to provide oxidation resistance to the super-alloy used as substrate (by serving as an Al reservoir), in addition to improving the adhesion with the top coat[17]. At the functional temperature, a bond coat should work to improve cooling air from the substrate without any reaction as well as melting[12]. The bond-coat is usually made of a MCrAlY where (M= Nickel or Cobalt or both). NiCrAlY (4 component) or NiCoCrAlY bond coats are deposited using different fabrication techniques which include Plasma-spray, HVOF or the EBPVD methods. Some further types of bond-coats are made of aluminides of Ni and Pt and are made by electroplating in unification with diffusion-aluminizing or CVD. In certain cases, the bond-coat consists of multilayers, having a dissimilar chemical/phase composition[18].

1.1.3 Thermally Grown Oxide (TGO)

Thermally Grown Oxide is a thin oxide layer (the thickness varies from 0.5 ~ 10 μm) that develops at the interface of the top coat (TC) & bond Coat (BC)[9]. The TGO is a result of the unavoidable interaction with the aluminum existing in the bond coat and oxygen passing from engine ambient through the top coat due to interconnected porosity present and also as it is porous to oxygen. TGO includes mainly Al_2O_3 and other oxides i.e. Cr_2O_3 , NiO, and (Spinel) $\text{Ni}(\text{Al}, \text{Co}, \text{Cr})_2\text{O}_4$ [15]. At optimum operating conditions in gas-turbine engines the temperature surpasses 700°C, which results in oxidation of the bond coat. Though the development of TGO is unavoidable, the bond coat is contrived so as to confirm the formation of TGO as $\alpha\text{-Al}_2\text{O}_3$ and that its development is uniform, sluggish and is defect free[19].

A uniform and dense α -Al₂O₃ layer can prevent the creation of TGO during oxidation due to ion diffusion. The growth process of α -alumina is either derived by inward oxygen diffusion or by outward aluminum diffusion through the TGO layer[20]. The addition of Al₂O₃ in YSZ improves the thermomechanical properties of TBCs and diminish the thermal expansion top coat interface mismatch[21].

1.1.4 Top Coat (TC)

The ceramic layer or top-coat is the top most layer of the TBC system which bears harsh and the high working temperatures in engines. It acts as an isolation layer to shield the super-alloy substrate against a thermal effect & diminishes the temperature of surface [22]. It has to fulfill certain requirements: (i) coefficient of thermal expansion close to the substrate, (ii) Elevated melting point, (iii) low value thermal conductivity, (iv) thermal shock resistance and (v) good oxidation resistance. Several ceramics have been applied as top-coat using modern techniques beside Thermal Spraying i.e. EB-PVD, CVD etc. Some of them are: Ca₂SiO₃, MgAl₂O₄ and CaTiO₃. However, Zirconia ceramics have been found most useful for use in harsh environments.

Best prevailing choice for top-coat material is (7YSZ or 8YSZ). Yttria stabilized Zirconia (YSZ) owns a suite of necessary properties that makes it one of the best material of choice for use as top-coat[23]. As it has lowest values for thermal conductivities at raised temperature of all ceramics ($\sim 2.3 \text{ W}\cdot\text{m}^{-1}\cdot\text{K}^{-1}$ at 1000°C for a fully compact material[24]. It also has low density and shock resistance properties[4, 21].

1.2 Applications of Thermal Barrier Coatings

Currently, Thermal Barrier Coatings are extensively used in:

- Turbine Blades[9, 16, 22, 23, 25]
- Aero-engine parts[7]
- Diesel engines[22]
- Combustion chambers[9]
- Shipboard Engines[7]
- Pressure Vessels[3]
- Exhaust Heat Management systems[5]
- High Temperature Operating Parts

1.3 High Entropy Alloys

High-Entropy alloys (HEA) are simply multi-component alloys comprising of 5 or more than five elements in moreover equi-atomic ratio or some near equi-atomic compositions [2]. Elements involved in this must contain a concentration ranging from 5 to 35 at %. HEAs can also contain minor alloying elements, in addition to the major alloying elements, each below 5 at. %. In this regard Zhou et al. in 2007 developed AlCoCrFeNiTi the first HEA by arc melting by varying the composition of Titanium and studied its mechanical properties and found that this alloy system shows best compression properties[26].

HEAs are named like this since their liquid or random solid solution states have ominously higher values of mixing as compared to the conventional alloys. Therefore, the entropy effect is much more distinct in the HEAs. Generally the development of intermetallic, brittle and complex phases is predictable to exist. All things considered, examinations have indicated the development of simple solid solutions having (FCC) face centered cubic and (BCC) body centered cubic arrangements due to the steadiness by high entropy effect[27]. No multifaceted or intermetallic phases were formed in this High Entropy Alloy system[28]. The rudimentary belief behind HEAs is that solid-solution phases are comparatively more stabilized by having considerably high mixing entropy comparatively than the intermetallic compounds, mainly at elevated temperatures.

1.4 Thermal Spraying

It is a group of coating procedures in which feedstock's which may be in form of powder or wires are heated and then projected on a prepared surface to be coated. The coating feedstock is heated by some electrical (arc or plasma) or by burning flame. It is a smart coating method as it offers a wide variety and selection of materials and processing techniques that includes ceramics, alloys, metals, plastics & in some cases composites. Feedstock in powder or wire form is excited to a molten or semi-molten form & then augmented towards substrate[5]. Thermal spray coating techniques such as Plasma spraying, flame wire spraying, HVOF, flame powder spraying, arc wire

spraying, & cold gas spraying, permit many corrosion, wear and thermal degradation issues to be resolved by using tailored coatings on surfaces. The basic principle of Thermal Spraying is illustrated in Figure 2.

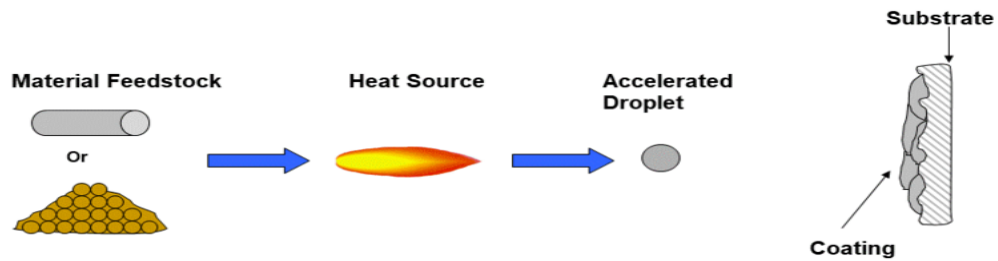


Figure 2. Schematics of Thermal Spraying

1.4.1 Atmospheric Plasma Spraying

Plasma spraying is widely used in coating industry. In this spraying method the material to be deposited (feedstock) is usually in powder or in some cases wire form, liquid or suspension. A DC arc is collide with (using typically on the order of 30V & 300 ~ 800A) amid the anode & cathode to produce plasma in the carrier gas, which is generally a mixture of Argon (Ar) plus Hydrogen (H₂) or He (Helium) & N₂[8]. A schematic diagram of a plasma spraying procedure is shown in Figure.3.

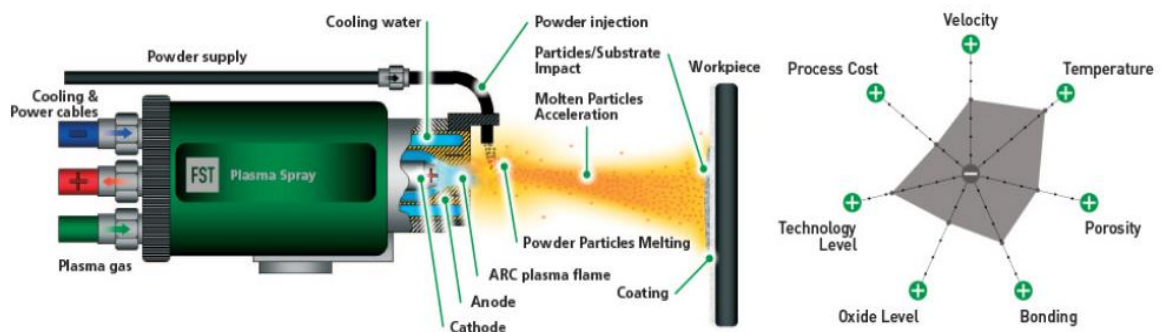


Figure 3. Principle of Plasma Spraying

The plasma jet temperature is on the order of approx. 16000 K. Feedstock is heated and projected to a coupon or substrate[29]. Semi-molten or Molten drops flatten,

promptly solidify and forms a solid deposit. Generally, the deposits stay adherent to the substrate as a coating. Free-standing coatings can also be manufactured by eradicating the substrate. A large number of technological parameters are involved which effect the kinetics of particles and therefore deposition properties. Feedstock nature, plasma gas composition and energy input, flow rate, torch offset or stand-off distance, substrate heating and cooling etc. are among these[8, 11]. Plasma Spraying is mainly used to deposit ceramics, metals, composites and certain other materials having high melting temperatures. Microstructure obtained by Plasma Spraying is fine with columnar boundaries. It has a high deposition rate $\geq 4\text{kg/hr}$. The bonding strength of the coating produced by APS has a metastable structure and is around 10~30MPa while porosity levels in the coatings is about 1~20% depending upon the stand-off distances and external environment[30]. The bonding strength for some of alloys of chromium, nickel and aluminum may reach up to 70MPa[31].

1.4.1.1 Components of Plasma Spraying

A Plasma Spraying system consists mainly of control unit, gas supply system, spray gun, water chiller, power supply, powder feeder, substrate holder and water jam box as represented in the figure below:-

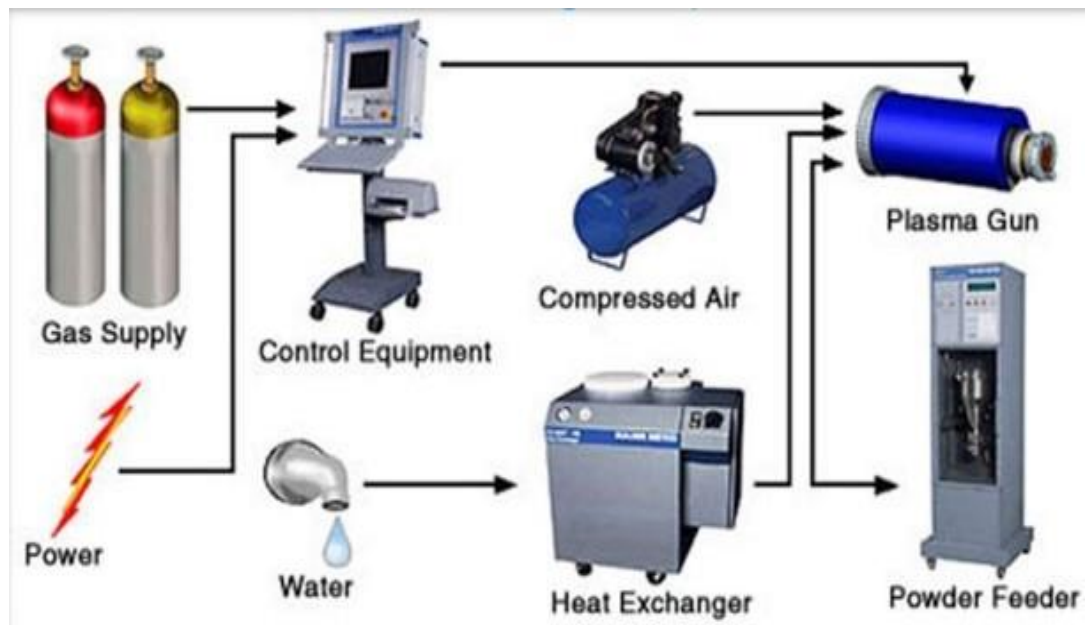


Figure 4. Schematic of a Plasma Spraying System

1.4.2 High Velocity Oxy-Fuel Spraying (HVOF)

HVOF is a thermal spraying technique in which a specially designed torch allows the compressed flame to expand freely consuming the gases combustion, such as Hydrocarbon's i.e. Methane (CH_4), Propane (C_3H_6), Butane (C_4H_8) or kerosene oil type liquid fuels. O_2 & fuel are mixed in the combustion zone under conditions that display the correct combustion mode & pressure. Nitrogen (N_2) is used as a carrier gas to propel the powder to the burning flame[12].

This process generates a very high velocity flame which is used to drive the particles at near supersonic speeds beforehand impact on the substrate[32]. The elementary rule of spraying is that elevated combustion pressure equals to high velocity of gas, high velocity of particles which results in high quality coatings. That is the reason why HVOF produce dense coatings than the APS technique.

The significant benefit of this process is achievement of high density coatings with low oxide content. The low oxides are partially due to the high speed of the particles spending less time within the flame and partially due to the lower temperature of flame (approx. $3,000\text{ }^\circ\text{C}$) of the flame as compared to alternative similar processes[33, 34]. Schematic diagram of HVOF spraying process is shown below.

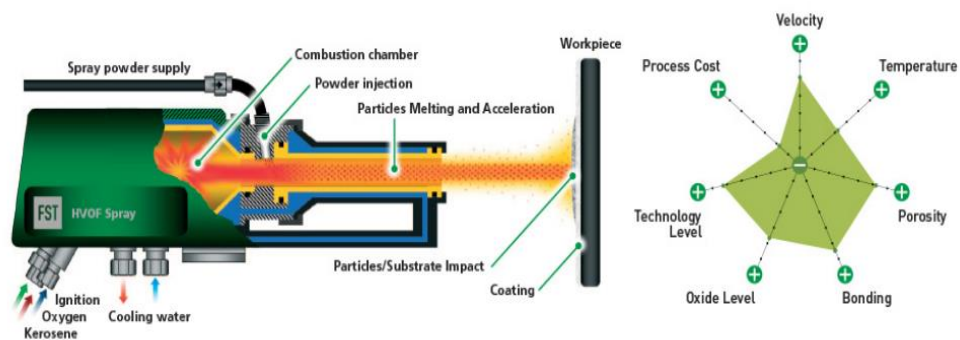
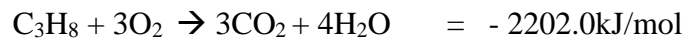


Figure 5. Principle of High Velocity Oxy-Fuel Spraying

A number of materials can be sprayed by HVOF spraying technique like soft metals, hard metals and their alloys and oxides. The choice of fuel or gas used is important while fabrication of a coating. Sometimes a higher temperature is required to soften the metal to be deposited. The stoichiometric balance is essential for proper

combustion and required temperature generation. For example in combustion of Propane as fuel the reaction takes place as following:-



The negative enthalpy of combustion in the above mentioned reaction shows that the reaction is exothermic in nature and a large amount of energy is released as the result of the combustion of frame which is used to melt the material in HVOF spraying.

1.4.2.1 Components of HVOF Spraying System

A HVOF Spraying system consists of control box, spray gun, water chiller, power supply, powder feeder, compressor, substrate holder and combustion gas cylinder[35]. It is symbolized in the figure below:-



Figure 6. Components of a HVOF Spraying System

1.4.3 Flame Spraying

This method of Spraying uses the combination of fuel gases and oxygen for getting temperature close to 2750°C. Propane, Acetylene, Hydrogen and Methane are commonly used fuel gases for combustion purpose, to melt wires or powders which are used are precursors for coating. Typically the particle velocity is about 40m/s and the deposition rate is 1 ~ 10 kg/h. Porosity level in the as-sprayed coating is 10 ~ 15%.

Chapter 2

Literature Review

Thermal barrier Coatings and High Entropy Alloys in recent years have drawn more attention from the researchers. Durability and life is the main problem of the TBCs besides this problem recent advancement in the materials and thermal spraying technology have been made which are discussed below to some extent.

Yeh et al. in 1996 for the first time gave the concept of High Entropy Alloy systems containing equal moles concentration[1].

Cantor et al. named the high entropy alloys as the multi-component systems in 2004 which led to the opening of new era for alloys development[2].

Meng et al. in 2018 studied the effect of controlled annealing for 10hrs in presence of Argon on commercially available CoNiCrAlY bond coats. The resistance to oxidation of the heat treated bond coat was as good as that achieved by (LPPS) Low Pressure Plasma Spraying[3].

Abbas et al. used finite elemental analysis method to estimate the stresses generated in YSZ/LaTi₂Al₉O₁₉ (LTA) double layer ceramic thermal barrier coatings having MCrAlY bon coat applied beneath the top coat[4].

Newaz et al. in 2001 reported that establishment and advancement of micro-decohesion is the main mechanism for failure of Thermal Barrier Coatings during thermal cycling tests[5].

Mendis et al. in 2006 studied the microstructure of as-coated as well as thermal cycled NiCoCrAlY bond coats. He found that NiCoCrAlY is not a single phased alloy system rather it have γ , β and σ precipitates in the entire bond coat[6].

Padtare et al. reviewed the use of Thermal barrier coatings in gas turbine engine applications in 2002 and also explained the anatomy of the thermal barrier coatings[7].

Löbel et al. in 2017 studied the processing of AlCoCrFeNiTi HEA by plasma spraying in which he used different feedstock materials. He declared the feedstock produced by inert gas atomization as best for wear resistance[8].

Cahit et al. in 2013 explained TBC systems and thermal cycle/shock behavior of TBCs under different service environments and the thermal cycle/shock tests used for evaluation of TBC systems[9].

F.Ghadami et al. in 2015 used WC-12wt%Co and NiCr as feed stock powders to produce conventional and NiCr/WC-Co doubled layer coatings and heat treated them 650~1150°C and concluded that adhesive strength increased with increasing temperature[10].

Anupam et al. in 2019 studied the microstructural evolution of equi-atomic AlCoCrNiFe mechanically alloyed powder coated by APS through extensive Microscopy[11].

Garcia et al. in 2018 studied the microstructure and effects of Tantalum (Ta) containing NiCoCrAlY coatings formed by HVOF spraying and concluded that Ta had an anchoring effect by inward diffusion[12].

Zhang et al. in 2010 investigated the effect of annealing on microstructure of CoCrFeNiCuAl HEA. Alloy was annealed for 2hrs at 1000°C and it showed high strength & excellent ductility in as-annealed state[13].

Vaidya et al. in 2019 reviewed the leading aspects of phase evolution, thermal stability, and different properties attained by the HEAs formed by Mechanical Alloying. The precincts and challenges of the method are also critically evaluated and also compared the consequences found after high-pressure torsion, alternative severe plastic deformation technique[14].

Zhang et al. in 2017 studied the non-parabolic oxidation kinetics of MCrAlY bond coats fabricated by (LPPS) low pressure plasma spraying. He found that TGO (Al_2O_3) have dissimilar oxidation rate constants when subjected to isothermal oxidations of longer intervals[15].

Avci et al. in 2018 studied the microstructure & oxidation behavior of Air plasma sprayed coatings. He concluded that after oxidation testing TGO formed at interface of Bond Coat and Top Coat led to the spallation of the Thermal Barrier Coatings[16].

Wu Kai et al. in 2017 studied the air oxidation of 3 different HEAs i.e. FeCoNiCrAl, FeCoNiCrSi & FeCoNiCrMn at a temperature range 700 ~ 900°C. The HEA FeCoNiCrAl showed the most oxidation resistant ability among the all tested HEA's[17].

Wang et al. in 2018 studied the microstructural properties of multilayer ceramic coatings on Steel 410, Graphite and Ti-6Al-4V substrates in order to provide a thermal barrier on diesel engine pistons to be operated at higher temperature. He also evaluated heat exchange between the layers and also observed the aging effect of as-sprayed coatings[18].

Di Ferdinando et al. in 2010 studied the isothermal oxidation resistance of commercial CoNiCrAlY bond coats developed by APS, VPS and HVOF Spraying. He found HVOF sprayed bond coats more oxidation resistant as compared to APS and VPS[19].

Huang et al. in 2009 deposited AlCrNbSiTiV nitride films on Si wafers by reactive magnetron sputtering and studied post annealing effects on the said films. Even vacuum annealing for 5hrs at 900°C didn't cause any notable change in the crystal structure[20].

Bai et al. in 2019 synthesized composite coatings having MCrAlY-Al₂O₃ by HVOF Spraying and found that these coatings showed better oxidation resistance than conventional MCrAlY coatings after being exposed to isothermal oxidation at 900°C for 10hrs[21].

Munawar et al. in 2016 studied the new type of top coats manufactured by EB-PVD process, on the bond coats as compared to the conventional YSZ and found that Gadolinium zirconate (GZO) has higher lifetime and thermal stability as thermal cycling was done at 1100°C. He also concluded that addition of 0.6% Hf increased the lifetime of the TBC system 10 times[22].

Munawar et al. in 2014 developed new TBC systems by studying different Nickel based super alloy substrates. IN100 was compared to CMSX-4. CMAS resistance as well as volcanic ash tests were done to test both types of superalloy substrates as well as TBC systems and also TGO growth was studied[23].

Afrasiabi et al. in 2008 studied the hot corrosion behavior of three different TBC systems i.e. YSZ, particle composite (YSZ+Al₂O₃) and layer composite (YSZ/Al₂O₃). He studied hot corrosion behavior of the said coatings at 1050°C for 40hrs and found that the system (YSZ/Al₂O₃) having layered structure resisted the hot corrosion to some extent[24].

Jadhav et al. in 2019 investigated FeCoCrNi₂Al, FeCoNiAlTi_{0.4}, FeCoCrNiAl_{0.3}, and NiCoCrAlSi (HEAs) manufactured by using Mechanical Activated route for potential bond coat usage in TBC systems. Amongst all studied HEAs FeCoCrNi₂Al showed best oxidation confrontation due to the development of α -Al₂O₃ layer[25].

Zhou et al. studied the mechanical properties of developed AlCoCrFeNiTi_(x) HEA by arc melting by varying the composition of Titanium and checked their mechanical properties and found that this alloy system shows best compression properties[26].

Meghwal et al. in 2020 published a review paper on the Thermal Spraying of HE alloys in which he discussed the formation and processing routes of these HE alloys. He discussed different feedstocks and microstructures of the HE coatings manufactured by several Thermal processing techniques. In this paper he also discussed oxidation behavior as well as the tribological behavior of some HE alloy coatings prepared by thermal spraying techniques[27].

Wang et al. in 2021 studied the mechanical properties as well as microstructure of AlCoCrFeNi HE alloys and post annealing affect at 600°C and 900°C. He concluded that the APS coating consisted of lamellar structure having BCC and FCC phases in it. BCC phase transformed into FCC at post –annealing stage and diffusion took place due to annealing[28].

Xiao et al. in 2020 manufactured FeCoNiCrMn coatings by Plasma Spraying with altering the H₂ flow rates. The increased flow rate of H₂ and subsequent annealing enhanced the wear and scratch resistance behaviour of tested coatings[29].

P Fauchais et al. in 2004 published his work in order to better understanding of plasma spraying process. He studied the plasma plume flame and the interactions with surrounding environment. He also summarized the melting behavior of the particles and the splat morphology formed upon the impact[30].

B. Garrido et al. in 2021 studied the in vitro characterization on 45S5 bio active glass coatings produced by plasma spraying. The prepared coatings were tested in vitro to estimate their behaviour by immersing them in imitation body fluid, Hank's Balanced Salt Solution. It was found that adhesion strength was increased for the plasma sprayed coatings of the heat treated samples[31].

Srivastava et al. in 2019 synthesized FeCoCrNi₂Al novel high entropy alloy coating by HVOF spraying and reported that coating was having major FCC phase while have some minor phase of BCC present. The prepared coating displayed good erosion resistance even at temperature of 800°C and thus is a suitable system to be used at high temperatures[32].

Richer et al. in 2010 studied the microstructure and isothermal oxidation of CoNiCrAlY bond coats developed by HVOF, APS and CGDS techniques and declared that low temperature technique GCDS is best for coatings having low oxide content[33].

Hsu et al. developed an overlay coating of NiCo_{0.6}Fe_{0.2}Cr_{1.5}SiAlTi_{0.2} having a BCC structure and containing much of Cr₃Si, which showed improved mechanical properties and better oxidation resistance like NiCrAlY coatings at 1100°C[34].

Karoglanli et al. led a comparative investigation of five HVOF sprayed coatings for wear and frictional behaviour. He used stainless steel substrates for spraying of coatings. He found that plastic deformation was found in Ni/Cr coatings while among all the five coatings under consideration WC/CoCr coatings showed best results for wear and friction behaviour[35].

Cheng et al. in 2019 studied the effect of phase changes during air plasma spraying of AlCoCrFeNi and also the effect of particle size on the phase changes. The BCC phase

was changed to FCC beyond 600°C and also degree of crystallinity augmented with increased annealing temperature[36].

C.Che et al. examined the effect of different bond coats roughnesses on lifetime of TBCs formed by air plasma spraying and concluded that the TBC having lesser bond coat roughness has greater lifetime duration than ones having more roughness[37].

Choi et al. in 2002 studied the isothermal oxidation of NiCrAlY i.e. Amdry 962 and Amdry 964 bond coats developed by air plasma spraying and declared Amdry 962 as more oxidation resistance than later one[38].

Anupam et al. in 2019 manufactured AlCoCrFeNi coatings by Cold Spraying and tested them for oxidation up to 25hrs at 1100°C and found satisfactory. He concluded that the diffusion is not slothful in the complex alloy framework of HEA[39].

Abhinay et al. in 2019 studied the high temperature oxidation behavior of Ni 30-Mullite coatings on mild steel coupons by HVOF spraying and reported that these coatings are stable at higher temperatures and thus can be used as high temperature resistant materials[40].

Tian et al. in 2016 studied the wear behavior and microstructure of mechanical alloyed AlCoCrFeNiTi High Entropy Alloy Coating by Air Plasma Spraying using mechanical alloyed feedstock. The HEA powder first consisting of single phase BCC transformed into FCC+B2+BCC and oxide phases upon AP Spraying[41].

Tianchen Li et al. in 2017 prepared FeCoCrNiMo0.2 coatings by both APS and HVOF techniques and studied their microstructure as well as wear behavior. The coating prepared by APS have more oxide content than HVOF spraying while the wear resistance of APS coating was higher than HVOF coating[42].

After reviewing the previously published work on the subject topic we can deduce that after the identification of HEA's in year 2004 by Yeh et al. and Cantor et al. several advancements have been made in this field. These HEAs and the alloy families were extensively studied in terms of their chemical, electrochemical and mechanical properties. They find applications as wear and corrosion resistant coatings and for protection of surfaces as well as sometimes used for some mechanical aspects. First of

all Plasma spraying technique was used to fabricate the HEA coatings as it is most flexible thermal spraying technique and different type and size of feedstock powders can be used . But owing to high plasma temperature oxidation of particles during flight occurs which forms oxide splats and causes porosity in coatings. On the other hand HVOF technique is comparatively better in terms of coating density as well as porosity. As the temperature of flame in HVOF is less so in flight oxidation (IFO) is minimized as compared to APS technique. Good quality coatings can be achieved by HVOF spraying. Cold Spraying is another less efficient technique than HVOF which doesn't require significant heating of feedstock. Other technique used is Laser Cladding in which blended or mixed powder is spread as bed and then focused laser beam is applied which melts the particles and form coatings. Vapor deposition or sputtering is also used to deposit HEA coatings but as it is a slow and expensive process so it is used at limited scale to form nitride/boride/carbide coatings having excellent tribological properties. Pre alloyed and Mechanical Milled/Alloyed powders are good for achieving the desired properties of the prepared coatings for specific applications while blended (mixed) powders require post coating treatments like vacuum annealing, Laser melting to form dense coatings upon melting due to high temperature of Laser. Among all different types of feedstock powders, pre alloyed gas atomized particles are the best feedstock to form good quality coatings because they have a spherical shape which is favored for high deposition rate and travelling through the spraying gun.

All the above mentioned already published work by several researchers on the HEA NiCoCrAlFe family reports multitude of phases with oxide stringers dispersed in the lamellar microstructure of coatings. FCC and BCC both are formed in different fractions resulting from the different spraying conditions as well as the used TS technique for fabrication of coating which is also depicted in our prepared APS coatings. The TS coatings prepared by different researchers using Mechanical Alloy (MA) powders used as feedstock revealed BCC phases, nanocrystalline in nature and Tungsten Carbide(WC) contamination which is then exhibited in the prepared thermally sprayed coatings along with oxide stringers.

After reviewing the already published work regarding our Alloy system and some similar type of HEA coating formed by different fabrication routes as well as the

powder feedstock manufacturing routes we suggest that pre alloying of alloy powder is a better option to be opted to avoid oxidation of powder during flight in the flame and we can use high deposition rate coating processes combined with post coating treatments like annealing and laser re-melting for achieving defect free and homogenized high entropy alloy coatings.

Chapter 3

Experimentation Methods

This section deliberates all the experimentation and processes involved in the fabrication of coatings. First of all we purchased elemental powders of Nickel, Cobalt, Chromium, Aluminum, Iron with purity > 99.5% from GREENEARTH CHEM West Nanjing Road, Shanghai, China and did Ball Milling for homogenous mixing of elemental powders. The apparatus used for the preparation of ball milled HEA powder and manufacturing of coatings was:-

- Beakers
- Sieve
- Spatula
- Poly Propylene Vial (1ltr)
- Steel Balls of Ø15 & 10mm (For ball milling)
- Vacuum Glove Box (To avoid oxidation of metallic powders due to atmospheric oxygen)
- Oven (For drying of powders)
- Weighing balance

3.1 Ball Milling (Mixing) of Elemental Powders

Above mentioned elemental powders having purity > 99.9 % were placed in a poly propylene vial in equi-atomic ratios in a Glove Box to avoid oxidation. After that stainless steel balls of Ø10 and Ø8 were inserted into the vial and Argon was filled in the vial to keep atmosphere inert during ball milling. Speed of the Ball mill apparatus was set to 110rpm and ball to powder weight ratio (mass ratio) was 10:1. Mixing of elemental powders was carried out for 10hrs in a 2-roll ball milling apparatus as shown in the Figure 7 in the Advanced Composites Manufacturing Lab at SCME.



Figure 7. Ball Milling (2-Roll) apparatus at SCME

3.1.1 Merits

- This is a simple and cost-effective method
- Excellent homogeneity
- Room-temperature technique
- Makes very fine powder (in some cases particle size $\leq 10\mu\text{m}$)
- Appropriate for milling noxious materials as it can be used in a closed container.
- Suitable for dry and wet milling

3.1.2 Demerits:

- Sometimes contamination of chemicals and particles occur
- Low efficiency
- High frictional loss of milled body
- Greater energy consumption

3.2 Samples Preparation for Coatings

In this process we have to prepare our substrate for coating purpose. We used Stainless Steel 316L as substrate material for coatings. As we know that in raw form steel is usually having grease or oil applied and has not much fine surface properties so we have to perform initial cleaning as much as it is possible.

3.2.1 Pre Surface Treatment

- a. **Cleaning process** was performed to remove any dust, oil, grease or any foreign particles present from the surface.
- b. **Shaping process** was done by cutting our samples into desired shape.
- c. **Surface activation** is performed by using different techniques like sand blasting and grit blasting as they enhance the surface roughness which in turn results in better adhesion of coating with the substrate. Other modern techniques for surface activation includes laser ablation and water jet treatment. In our experiment we used grit blasting to prepare our substrates for coating purpose.

Shaping was done using a diamond cutter and also **Electrical discharge machining** (EDM) also known as **Spark Machining**. The substrates were cut into 1inch x 1inch dimension from a blank. After that cleaning was done by dipping the substrates in acetone (CH_3COCH_3) to remove impurities and dirt.

3.2.2 Grit Blasting

To increase the surface roughness of our shaped substrates I did grit blasting at pressure of 0.35MPa followed by air drying. Alumina (Al_2O_3) particles having particle size of 40~60 μm was used for grit blasting. Air drying is done to remove any stuck particles or dust to the substrate surface. The pressure for air drying must be slight lower than the pressure used for grit blasting because it can cause alteration of the prepared surface.

Table 1. Parameters for Grit blasting

Compressor	Grit blasting intake	Blasting Pressure	Angle
0.50MPa	0.40MPa	0.35MPa	60°

As power is given compressor starts running and generates pressure. We set up the value to 0.5MPa. When the set value is achieved the compressor starts automatically. The compressed air is then sent to the dryer where water vapors are removed and then it is sand to the grit blaster. We have to wear proper safety gear to avoid any havoc or health issues. Safety at this stage is especially related to inhaling because alumina particles or sand in case of sand blasting can cause severe respiratory issues. Proper

movement of the blasting gun is required in order to ensure uniform layer development and surface roughness.

3.2.3 Pre-heating of Substrates and Powder

Pre-heating of the ball milled High Entropy powder as well as the substrates was done in order to remove any moisture present. Pre-heating of the processed HE powder was done by placing it in the oven for 2 hours at 25-150°C. HE powder was placed in a bowl and was covered with aluminum sheet to avoid any vaporization towards the oven wall. The substrates were pre-heated with the flame of spray spraying gun by closing the powder feeder.

3.3 Atmospheric Plasma Spraying Coating of Samples

All four type of samples with different stand-off distances i.e. 200mm, 250mm, 310mm and 370mm were manufactured by means of a conventional Atmospheric Plasma Spraying system (Metco 9MC, Sulzer Metco Inc Westbury, New York USA) as shown in Figure 8.

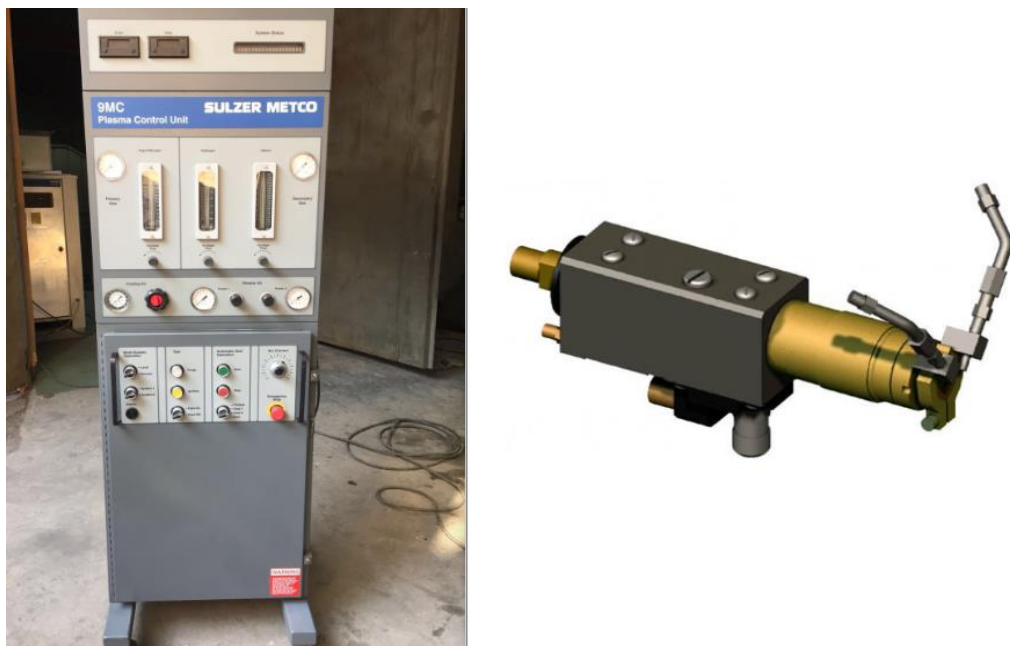


Figure 8. Atmospheric Plasma Spraying System: 9MC Controller & 9MB Nozzle

Argon (Ar) gas was employed as the primary plasma operating gas and hydrogen (H₂) was used as the secondary gas to escalate the whole plasma jet temperature. The feedstock ball milled powder was conveyed by a separate argon source and inoculated

superficially into the spawned plasma jet at an angle of 90 degree with reference to the anode axis. After that plasma torch assembly was mounted onto a robotic arm (YR-SK16-J00 Motoman, Yaskawa Electric Corp, Japan) to navigate across the substrate holders for coating. All the parameters of the plasma spraying operation are enlisted in Table 2.

Table 2. Plasma Spraying Operating Parameters

Sr No.	Parameters	Value
1	Arc voltage (V)	70
2	Arc current (A)	600
3	Powder Feed rate(g/min)	30
4	Primary Gas Flow (Ar/slpm)	40
5	Secondary Gas Flow (H ₂ /slpm)	2
6	Powder Feed Gas Flow (Ar/slpm)	5
7	Stand-Off distance (mm)	200, 250, 310, 370
8	Traverse speed of torch (mm/s)	200
9	Angle	90°
10	Nozzle Type	9 MB
11	Controller	9 MC

3.3.1 Merits:

- A widespread variety of coating feedstock materials for versatile applications, with almost all type of materials available in a suitable form.
- Several types of material, containing metals, ceramics, plastics, glass, and composite materials can be used as substrate for coating.
- The high temperature of a plasma jet makes it predominantly appropriate for coating of refractory metals as well as ceramics, including Zirconia (ZrO₂), Boron Carbide (B₄C) & Tungsten etc.
- A wider particle size powder range can be used as feedstock, typically 5-100µm, in contrast to HVOF spraying.
- It is a widely available & well-established coating process that is well renowned.

3.3.2 Demerits:

- Much Expensive
- Line-of-sight procedure, making it problematic to coat internal bores of very minor diameters and limited access surfaces.
- Not suitable for manual operations
- High temperatures can lead to more oxidation

3.4 Annealing of Coatings

After the fabrication of APS coatings the annealing was done for 4hrs duration at 1000°C for homogenization of the prepared coatings microstructure in a Tube Furnace held at Heat Treatment Lab of SCME and is shown in figure below.



Figure 9. Tube Furnace at Heat Treatment Lab SCME (NUST)

3.4.1 Aims and Objective

This study aims to develop high entropy alloy bond coat for gas turbine blades application. This study includes:

- Synthesis of High Entropy Alloy Powder
- Investigation of the Corrosion Behaviour of prepared alloy coatings
- Furthermore, these bond coats can be employed for protection of other structural parts operating at high temperatures.

Chapter 4

Characterization Techniques

4.1 Scanning Electron Microscope (SEM)

It is a characterization technique in which a fine beam of electrons is engrossed over a specimen's surface. Photons or Electrons are knocked off from the material's surface resultantly. These knocked off electrons are then focused onto the detector. The output from the detector controls the brightness of the cathode ray tube (CRT). For every point where the electron beams are focused and interact, it is plotted on consequent point on CRT and the material's image is produced[43].

The electron-surface interface causes the discharge of secondary electrons (SE), backscattered electrons (BSE) and X-rays[44]. Common mode of SEM for detection is by secondary electrons. These electrons are emanated from near the sample surface. So, a distinct and vibrant image of the sample is attained. It can divulge sample details even less than 1nm in size. Elastic scattering of incident electrons also takes place and release back scattered electrons. They emerge from deeper locations as compared to secondary electrons. So, their resolution is comparatively low. When an inner shell electron knocks off from its shell it emits characteristic x-rays[45].

We use SEM as it has easy sample preparation and we can figure our sample's morphology, chemistry, crystallography, and orientation of planes. Magnification of SEM can be controlled from 10 to 500,000 times.

Microstructure and cross section analysis of the all prepared coatings in as-coated condition were performed on Leo Gemini Analytical SEM at DLR Germany and annealed conditions were examined on (JEOL-JSM- 6490LA) and VEGA 3. Elemental composition was determined by EDS detector attached to Leo Gemini SEM at DLR Germany. BSE imaging analysis of the coatings which were subjected to the isothermal oxidation testing for 5, 15, 50 & 100hrs was carried out by using MAIA3 TESCAN SEM at Bartin University Turkey.

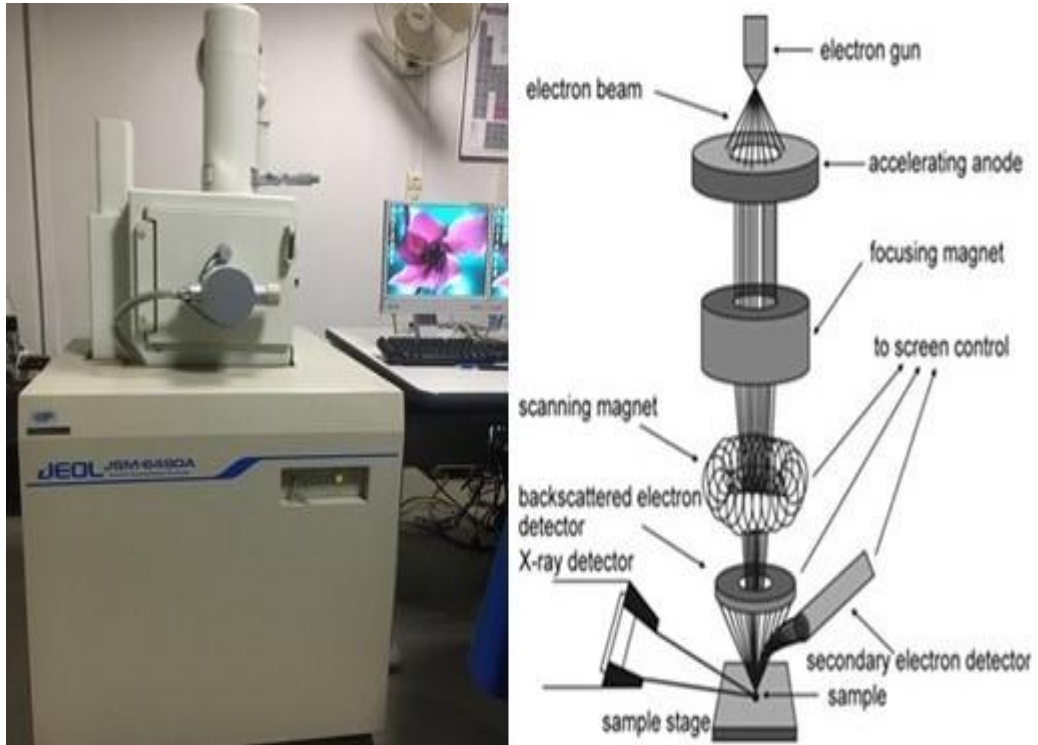


Figure 10. (a) JOEL JSM-6490LA SEM at SCME; (b) Schematics of SEM

4.2 X-ray diffraction (XRD)

It is used for the elucidation of the crystal structure of the material. It is a non-destructive technique, and it delivers fingerprints of Bragg's reflections of crystalline materials[46]. It contains 3 main parts. A cathode tube, a sample holder and detector. X-rays are produced by heating filament element which accelerates electrons towards a target which collide with target material with electrons. As a crystal is composed of layers and planes so, x-rays which have wavelength similar to these planes is reflected at that angle of incidence which is equal to the angle of reflection. "Diffraction" takes place and it can be described as by Bragg's Law:

$$2d\sin\theta = n\lambda \dots\dots\dots (4)$$

Constructive interference takes place when Bragg's law satisfied and "Bragg's reflections" will be picked up by the detector. These reflections positions tell us about inter-layer spacing-ray diffraction tells us about the phase, crystallinity, and sample purity. By this technique, one can also determine lattice mismatch, dislocations, and unit cell dimensions.

X-ray diffractions were accomplished by using STOE diffractometer at XRD Lab SCME-NUST. The scan angle was taken in 2θ and samples were scanned from 20° to 80° with a scan rate of 0.02° .

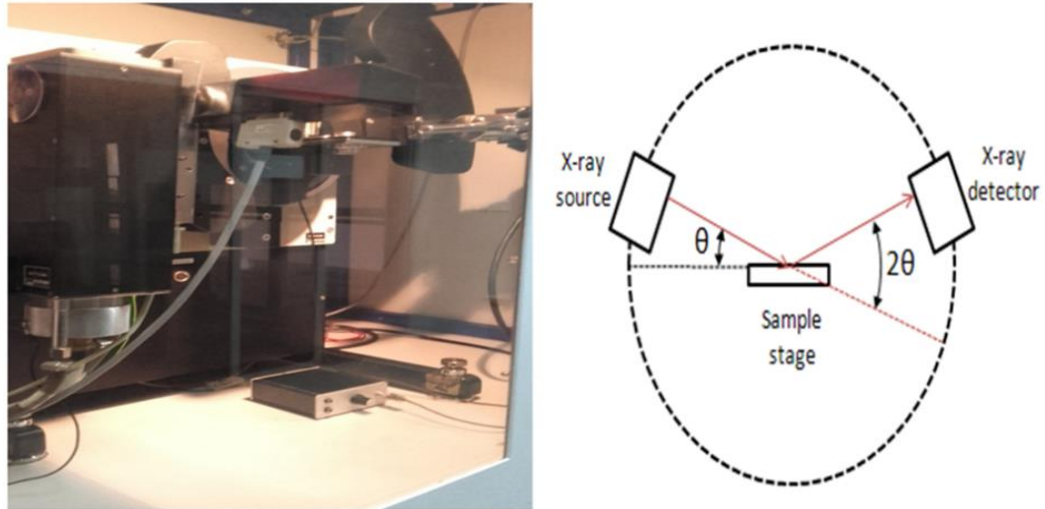


Figure 11. XRD present at SCME- NUST (b) XRD basic schematics

4.3 Hardness Testing of Coatings

Hardness is the measure of the ability of a material to resist deformation when certain loads acts upon it. It is done in accordance with a standard test procedure in which resistance of surface to the indentation is measured. Hardness depends upon the load applied while testing. The type of hardness test done depends upon indenter: Rhombus shape of indenter is in Knoop test, Square shaped indenter in Vickers test and triangle shaped in Berkovich pyramid. For carrying out hardness measurements of prepared as well as annealed coatings proper polishing and grinding of the cross section is required after proper mounting them. Micro hardness testing was done at Bartin University for the as-coated and annealed substrates using a micro tester (Duramin, Struers, Denmark). Micro hardness of SS316L was carried out at SCME.



Figure 12. Micro Hardness Testing equipment at SCME

4.4 Roughness Testing

A surface roughness tester is usually used to check the surface quality or roughness of a material. It displays the measured roughness depth (Rz) & the mean roughness (Ra) in microns (μm). Surface Roughness is also checked by using manual comparison using a "roughness comparator" (a known surface roughness sample) which is mainly used for checking the surface finish or roughness of the parts made by machining processes i.e. turning and milling etc. The surface being checked is matched with the surface roughness/finish comparator and then quoted but more commonly a surface profile quantification is made with a profilometer. We used a surface roughness tester (SE 700) of Korean Origin to measure the surface roughness of our substrates in different states i.e. bare stainless steel, as-coated and in as- annealed form.



Figure 13. SE700 Roughness Tester

Chapter 5

Results and Discussions

After the fabrication of coatings by APS, XRD analysis for identification of phases and SEM analysis for the microstructural studies was carried out followed by Surface Roughness measurements in both i.e. as-coated state as well in the annealed state. After that micro hardness tests were done through the grinded and polished cross sections of the fabricated coatings in both the states. Corrosion Behaviour as well as hot corrosion behaviour of the coatings was checked. Isothermal Oxidation Tests were performed on the annealed coatings.

5.1 XRD Analysis for Phase identification

XRD analysis was done for the phase identification and crystal structure of the present compounds of the High Entropy coatings. XRD analysis was done at all stages and in all states i.e. in as-coated, as- annealed states as well as after the isothermal oxidation testing of the respective Coatings.

5.2 As-Coated High Entropy Coatings

XRD analysis of the APS sprayed substrates in the as coated conditions revealed BCC and FCC as the major phases or we can say that a multitude of BCC & FCC phases was detected. It can be seen that as-sprayed coatings mainly consists of pure metals having BCC and FCC crystal structure, except some quantities of Fe-Cr, FeO and spinel formation which can be elucidated from XRD peaks shown below. In tallying, due high plasma jet temperature in-flight oxidation occurs in APS process peaks of mixed spinel oxides which are (marked : ♠) AB_2O_4 (A= Ni/Co/Fe, B=Al/Cr) were also detected.

All the diffraction peaks correspond well with the already published work[47] as we don't have known accepted patterns or reference cards for the concerned alloy and alloys system. The Crystal structure belongs to the cubic system. Major peaks representing the BCC & FCC are found to be present. Some of the Diffraction peaks are slightly shifted in comparison to already published work on this alloy system

because of Low Energy Ball Milling of our elemental powders which doesn't make HE alloy at the Ball Milling stage and also difference in the atomic radii of Ni, Fe, Cr, Al and Co.

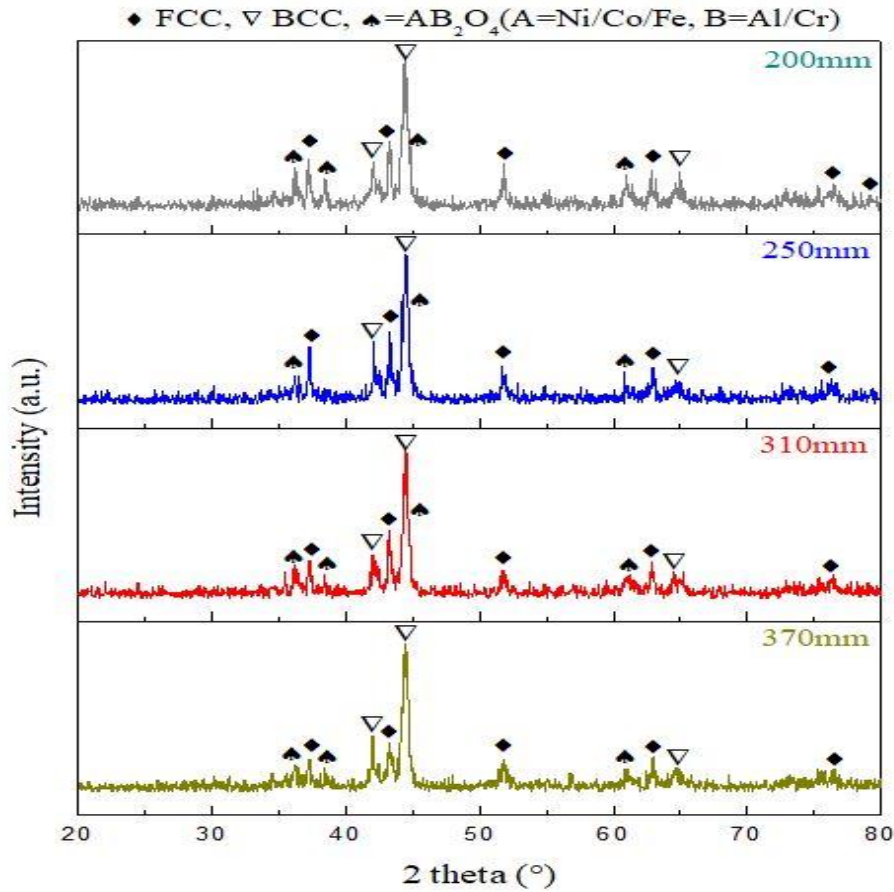


Figure 14. XRD analysis of the coatings in as-coated condition

5.3 As-Annealed High Entropy Coatings

High Entropy APS coatings were successively annealed at 1000°C for 4 hours in a tube furnace at SCME having inert atmosphere containing Argon (Ar) and XRD analysis was done after the Vacuum annealing treatment. After the annealing at 1000°C the content of Cr-O increased in the coatings while the presence of pure metal content minimized, similarly found by Lin et al. [47]. Due to heat treatment at 1000°C for 4hrs the elemental diffusion took place to a larger extent sufficiently which enhanced the entropy of our system significantly and restricted the formation of the intermetallic compounds which are the ordered phases.. The increase in the entropy of the system reduced the free energy of the alloy system thus, making stable solid solutions. It revealed BCC and FCC as the major phases present in the coating

microstructure. Some peaks of mixed spinel oxides which are (marked as S) AB_2O_4 (A= Ni/Co/Fe, B=Al/Cr) were also detected which is due to the in flight particles oxidation owing to high temperature of Plasma found prior in as-coated condition. The Crystal structure belongs to the cubic system. Major peaks representing the BCC & FCC are found to be present. Some of the Diffraction peaks are slightly shifted from their position from the XRD Diffractogram of as coated states. Like the intensity of the Peak at 2θ value of 37.16° increased. The peak for spinel at 2θ of 38° changed to FCC, the peak at 2θ value of 41° is divided into three smaller peaks for BCC, FCC and Spinel as well. The peak of BCC structure present at 2θ value of 42° disappeared. This all phenomenon is due to the fact that by annealing treatment of our Plasma Sprayed coatings in the inert atmosphere leads to the formation of High Entropy Alloy formation by slow diffusion of atoms with each other which was not achieved at the low energy ball milling stage.

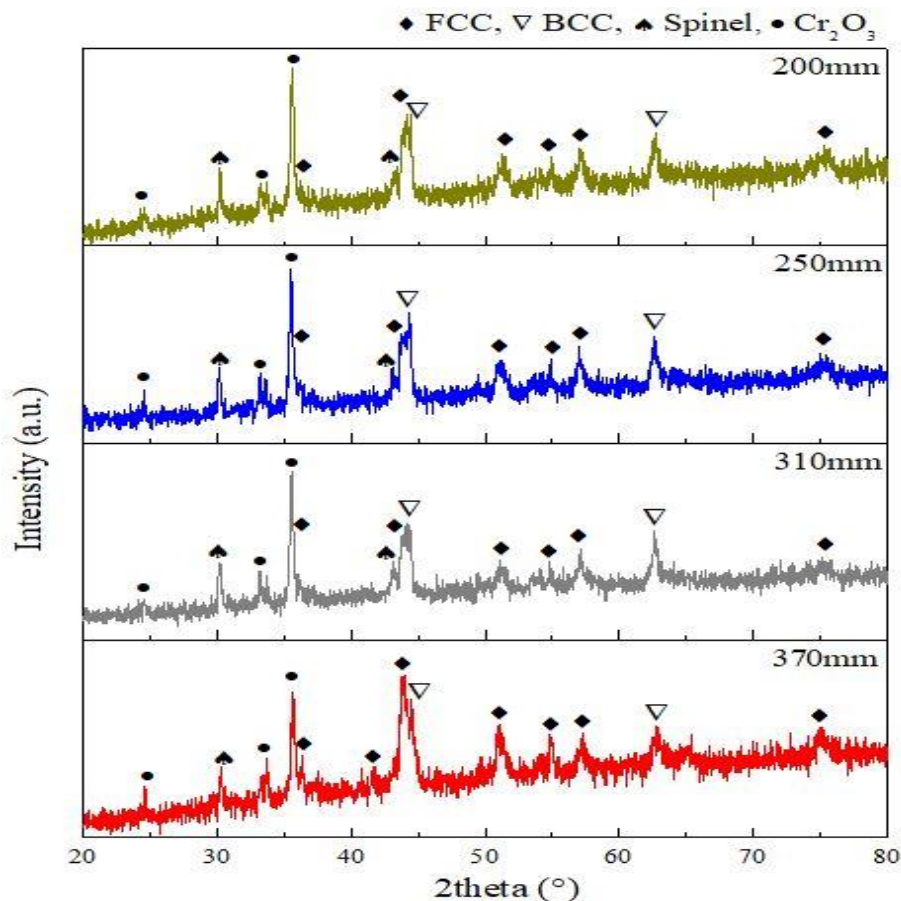


Figure 15. XRD analysis after annealing of coatings

5.4 After Isothermal Oxidation Testing

Oxidation testing of the annealed coatings was performed in the Heat Treatment Lab at SCME in a Nabetherm Furnace at a temperature of 1000°C for 5, 15, 50 and 100hrs. It was found that for the duration of 5hrs oxidation testing the xrd peaks show no significant changes from its annealed structure but some phases were changed a little to HE alloy phase after 15hrs oxidation testing. Now XRD pattern for oxidation testing duration for 50hrs revealed formation of α -Al₂O₃, Chromia (Cr₂O₃), NiO, fcc and small amount of Spinel (AB₂O₄) formation. The isothermal oxidation testing for 100hrs duration shows that mainly α -Al₂O₃ is formed along with NiO, AlN₃,fcc, and Cr₂O₃.

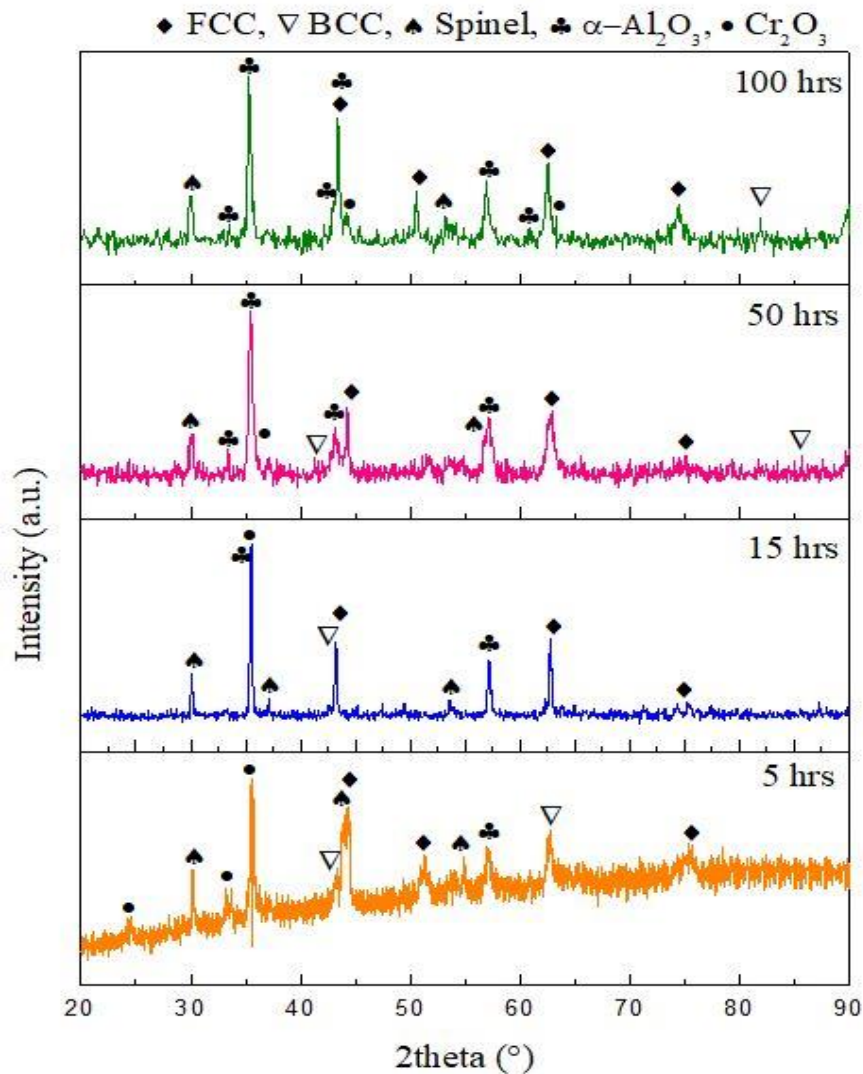


Figure 16. X-ray diffraction results after Oxidation Testing

5.5 SEM Analysis of Coatings (Microstructure Studies)

SEM analysis of the High Entropy Coatings were carried out at all stages of fabrication as well as testing.

5.5.1 SEM analysis in as-coated condition

Microstructure and Cross-Section of the prepared Thermal Barrier Coatings was examined by Analytical Scanning electron microscope (JEOL6490A) at SCME and also at the German Aerospace Centre (DLR) by Leo Gemini .SEM analysis of the coatings show the splat morphology and microstructure from. SEM images of coatings cross section in the as-coated condition are shown in the Figure 17.

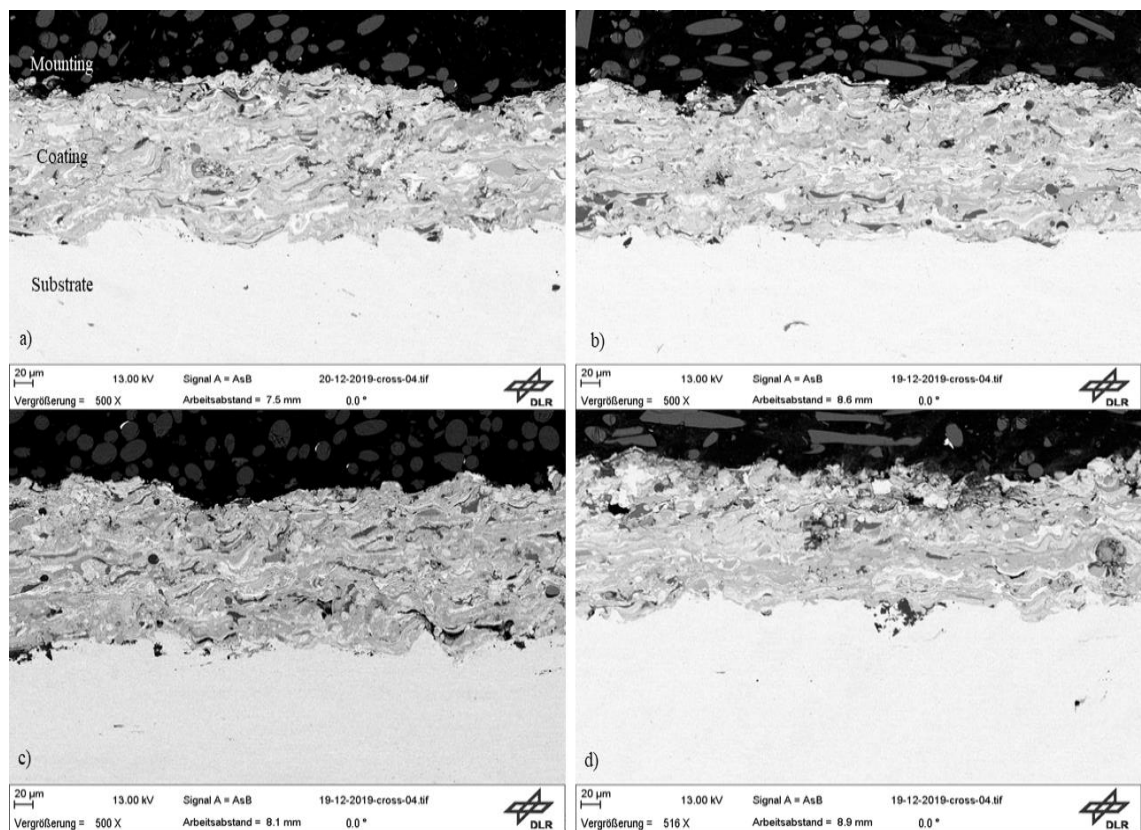


Figure 17. SEM micrographs of Coatings in as-Coated condition with varied Stand-off distances a) 200mm b) 250mm c) 310mm and d) 370mm

It can be clearly seen by viewing the SEM images that the Coating exhibit the splat morphology containing dark and light phases. Due to high temperature of Plasma torch maximum powdered particles are melted and formed splats morphology while some of them which experienced lesser temperature adhered to the substrate in a partially molten state. It is homogeneous and well adhered to the Stainless Steel substrate

having an average thickness of 150 ~ 180 μm . Overall the coating deposition efficiency was good and a continuous coating was achieved. The coating morphology shows some pores, micro cracks, voids and the lamellar structure as shown below.

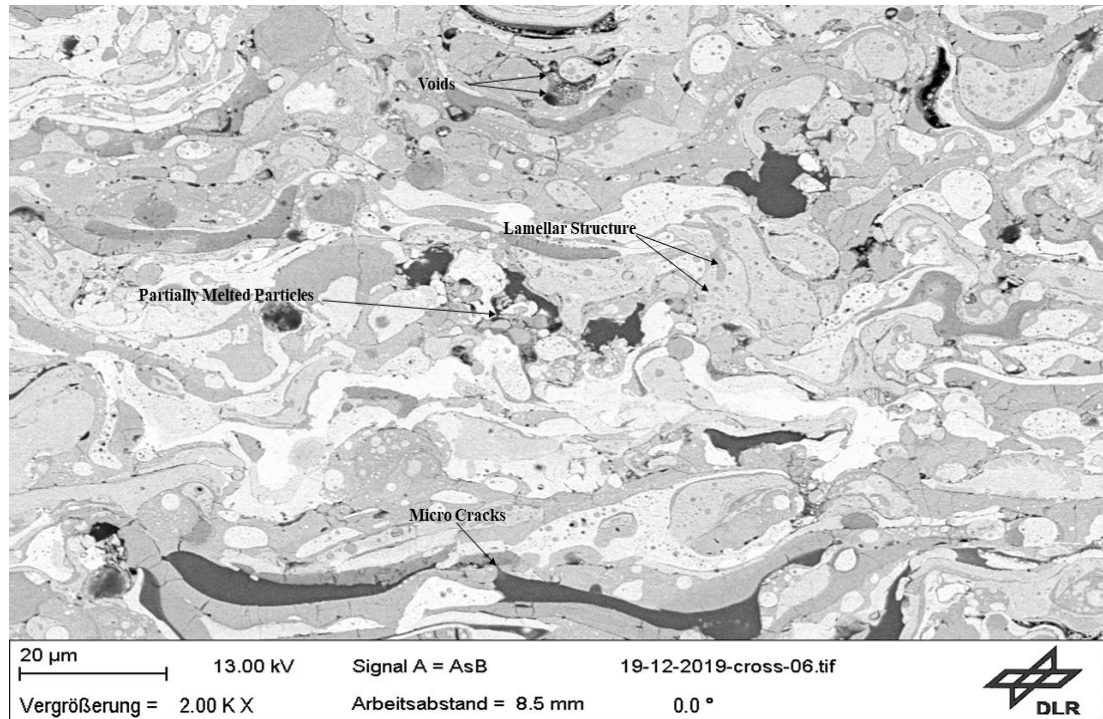


Figure 18. Enlarged view of the as-coated Microstructure

5.5.2 SEM analysis in as-annealed condition

After the fabrication of APS coatings the annealing was done for 4hrs duration at 1000 $^{\circ}\text{C}$ in presence of inert atmosphere in a Tube Furnace at Heat Treatment Lab of SCME. After that Microstructure studies were carried out at cross section using a VEGA3 TESCAN SEM. The microstructure of the annealed coating revealed a lamellar structure just like it was in its as-coated form but there was a major change observed after annealing treatment of the spayed substrates. Three types of phases were detected on the basis of color contrast i.e. Dark Gray Phase, Light Gray Phase and White Phase (HEA) as reported earlier by Meghwal et al.[48].

Dark Gray Phases were hard and consists mainly of spinels, and other oxides solidified after plasma spraying while the white phase is the soft phase as compared to the other two light and dark gray phases and is solid solution which is actually the High Entropy Alloy[27]. As we annealed the samples in inert atmosphere it can be

seen that the white phase fraction increased which is evident from the SEM images of the annealed samples which is the proof of HE alloy formation after post heat treatment (annealing) of the plasma sprayed coatings.

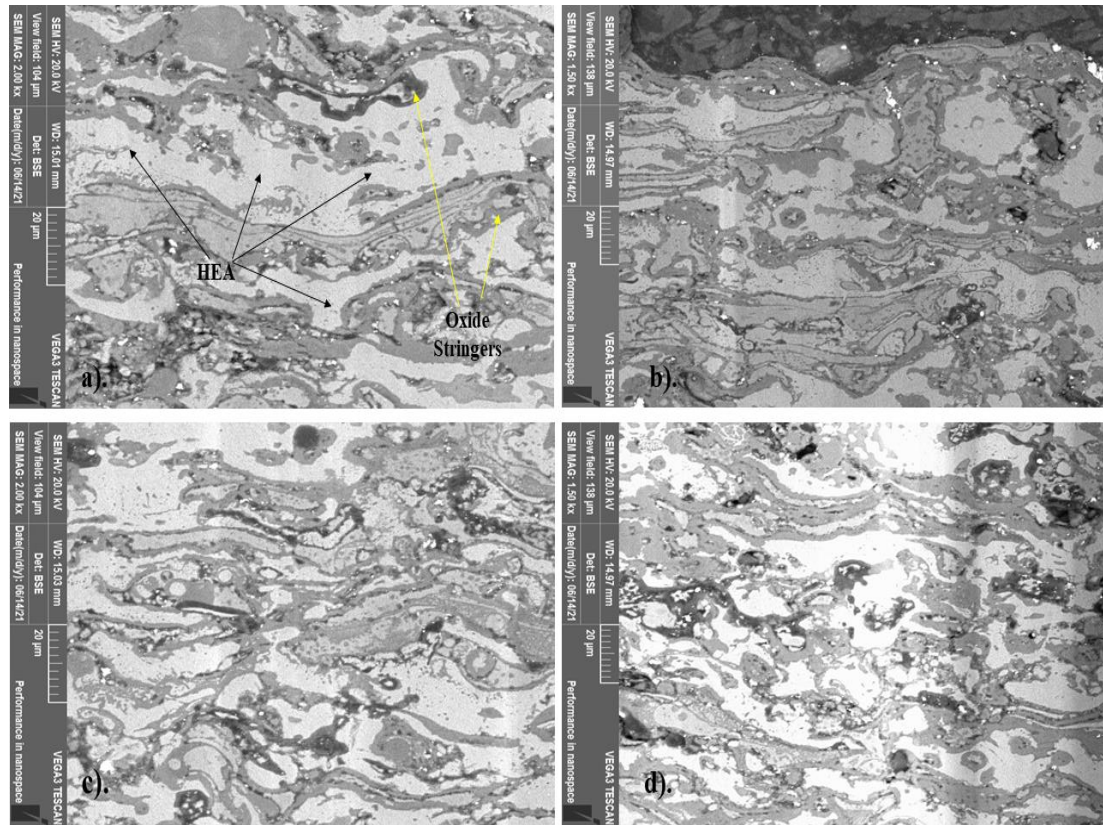


Figure 19. Microstructure of Annealed Coatings at 1000°C for 4hrs a). 200mm, b). 250mm, c). 310mm and d).370mm

Alongside the HE alloy fraction we can see oxide stringers which appeared as light and dark grey phases which is the inherent or obvious owing to the much high temperature of plasma flame due to which these oxides are formed and are a part of the sprayed coating as seen in the microstructure of above annealed coatings. The annealing at 1000°C for the stipulated time was enough for the diffusion of atoms into each other to form HE alloy which was not achieved prior completely. The presence of Argon gas halted any oxide formation while carrying out annealing and facilitated the diffusion of elements for the formation of alloy phase which can be seen in the SEM images.

5.6 SEM analysis after oxidation testing of coatings

Isothermal Oxidation behaviour of the prepared coatings was investigated in order to evaluate the thermal stability and check the TGO formation on the bond coat. The Samples were kept in a furnace at 1000°C for different time durations i.e. 5, 15, 50 & 100hrs and were examined by BSE SEM after proper grinding and polishing of the cross sections of coatings.

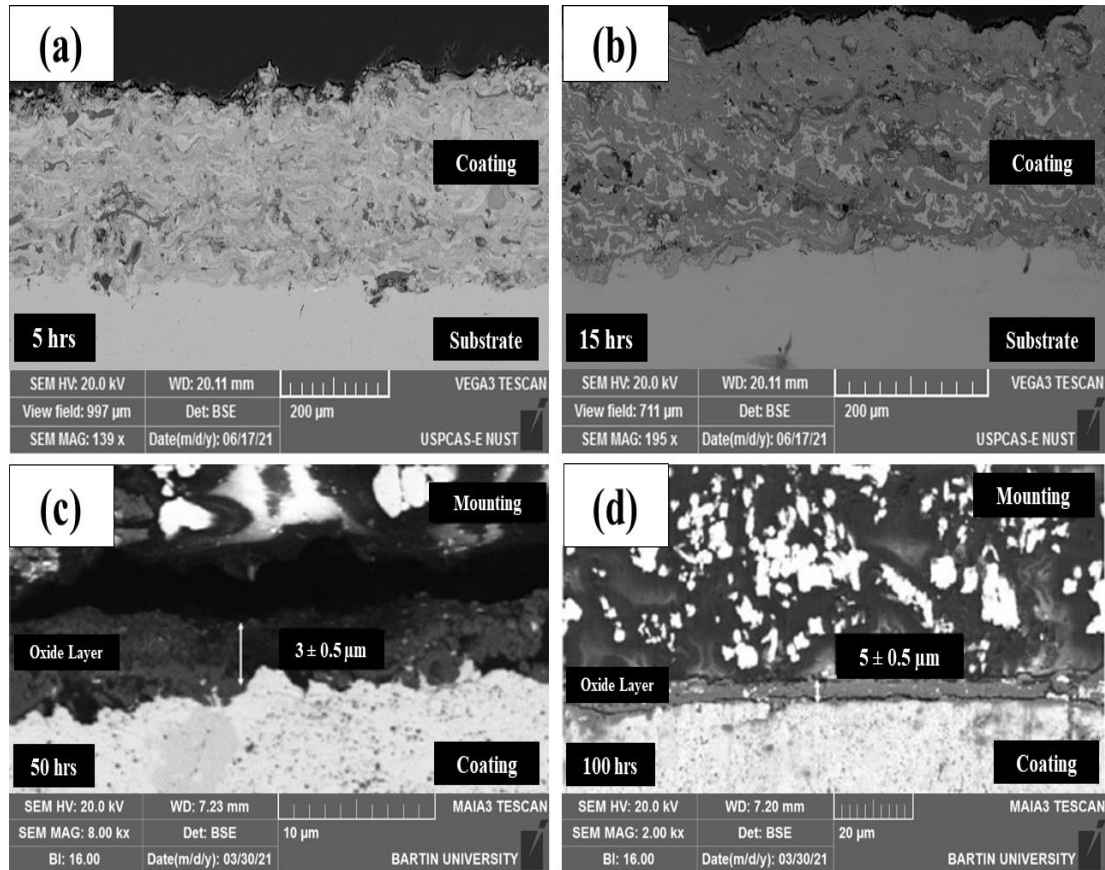


Figure 20. SEM images after Isothermal Oxidation Testing of coatings for a) 5hrs, b) 15hrs, c) 50hrs & d) 100hrs duration

It was found that for the duration of 5hrs oxidation testing the xrd peaks shows no significant change from its annealed state but some phases were a little microstructure was changed depicting the formation of spinel, chromia and HE alloy phase after 15hrs oxidation testing. No continuous TGO growth was observed after 5hrs and 15hrs oxidation testing. The XRD pattern for oxidation testing duration for 50hrs revealed a TGO layer which consists of α -Al₂O₃, Chromia (Cr₂O₃) as well as small amount of Spinel (AB₂O₄) structures and having an average thickness of 3±0.50µm. The

isothermal oxidation testing for 100hrs duration shows that a well observed TGO layer having an average thickness of $5\pm 0.50\mu\text{m}$ is observed $\alpha\text{-Al}_2\text{O}_3$, fcc, and Cr_2O_3 XRD peaks were observed. The TGO growth is well formed and is continuous on the bond coat after these long durations for oxidation testing of annealed coatings.

5.7 Micro Vickers Hardness

We can define hardness as the capability of a material to resist the localised plastic deformation[49]. Four tests were performed for each sample and readings are recorded as average. Proper grinding and polishing is required for sample preparation to do hardness testing of samples[50]. While performing the heat treatment of our samples at elevated temperatures of 1000°C we had a greater extent of elemental diffusion. As there was somewhat random distribution of different mixed elements oxide stringers were also formed in the microstructure which can be deemed as a possible reason for high hardness value. While in case of annealed coatings it is evident that high entropy alloy is formed, which decreased the free energy of the coatings. We can conclude that solid solution was formed after annealing, which increased extent of lattice distortion and inhibited dislocation motions is responsible for higher hardness values of the annealed coatings as compared to the as-sprayed coatings.

Table 3. Hardness Measurement Values

Load	Dwell Time	Micro Vickers's Hardness (HV)		
		SS 316L	Coated	Annealed
100gm	15 sec	490.15 HV	288 HV	345

Results for the micro hardness value of Bare SS 316L , APS coating and annealed coatings are also shown graphically below:-

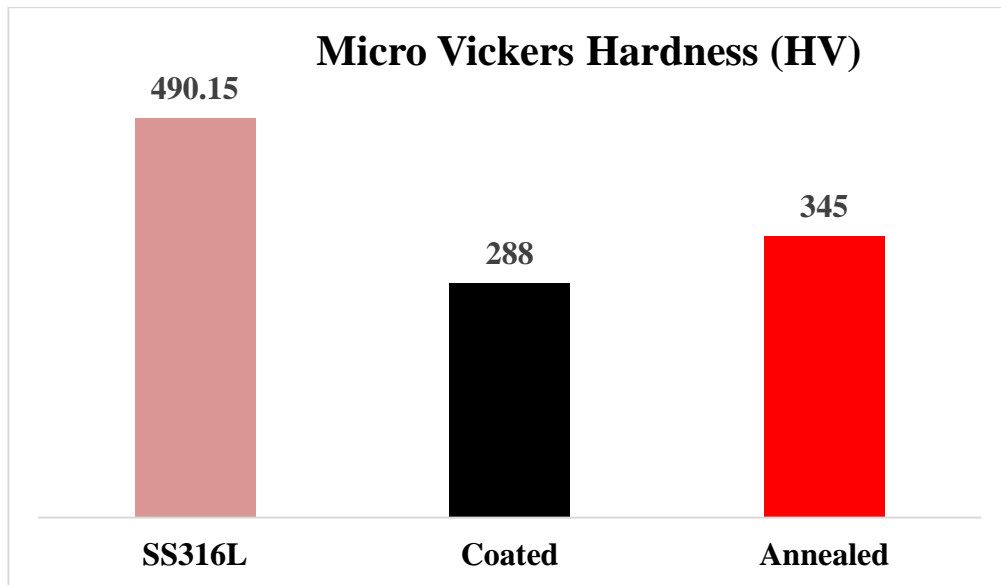


Figure 21. Micro Hardness Values of SS 316L, APS Coating and Annealed Coating

5.8 Roughness Testing

The surface was prior cleaned for the examination so that we may get true values for our observed roughness values of our different samples. Four readings were done and then average was taken for each coated sample. Roughness values for different samples is summarized below in the table.

Table 4. Roughness measurements of coatings

Sr No.	Sample	Ra (μm)	
1	SS 316L Substrate	2.274 (avg)	
2	Coated	200mm	7.124
3		250mm	7.167
4		310mm	7.478
5		370mm	7.497
6	Annealed	200mm	6.681
7		250mm	6.695
8		310mm	6.729
9		370mm	6.741

After observing the roughness values of the samples as a function of the spraying distance and subsequent annealing them we can propose that while we increased the

spraying distance the roughness values of the coatings were found to be enhanced. By this we can infer that while the distance was increased the particles were found in molten & semi molten forms which adhered to the substrate in the form of coating. As soon as we annealed the coatings the roughness began to lower as the temperature applied in annealing favoured the alloy formation and due to the diffusion of particles the surface roughness was lowered as compared to their respective coatings. The results are also summarized below in the graphical form.

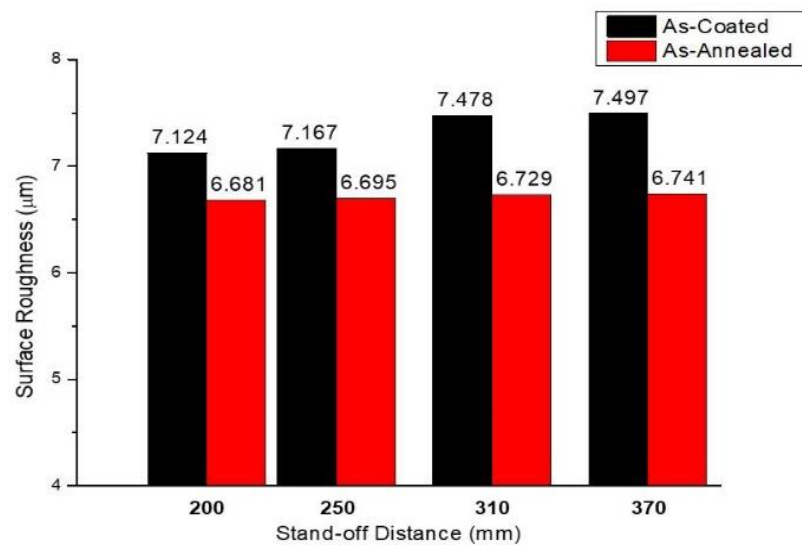


Figure 22. Surface Roughness

5.9 Potentiodynamic/Corrosion Behavior Testing

Corrosion or Potentiodynamic testing is done in order to check their response and corrosion behaviour efficiency of the materials in different environments[51]. Julius Tafel (1905) gave the experimental relationship between the Current (I), and the over-potential (η). He was testing electro catalytic behavior of different electrode including Tin, Mercury, for reduction reaction of hydrogen.

$$\eta = a + b \log I$$

Where, the η is over-potential and can be referred as the difference between potential of working electrode and equilibrium potential. There is linear relationship between working electrode potential and log of current only if electrodes are polarized at adequately immense potentials and away from both anodic and cathodic corrosion potential in both directions. To evaluate the experimental data, I_{corr} is evaluated using

Tafel extrapolation by plotting a graph between equilibrium potential E versus \log of I_{corr} curve. A potential scan of almost ± 300 mV about E_{corr} which is generally required to determine if a linear section of at least one decade of current is present, this perfect extrapolation can be done to E_{corr} potential. The corrosion current density is calculated by dividing I_{corr} by the specimen area.

$$i_{\text{corr}} = \frac{I_{\text{corr}}}{A}$$

The curves obtained by anodic polarization are not used owing to fact linear region over at least one decade is absent for many alloys and metals showing exhibit active passive behavior[52].

In the current studies corrosion testing was carried out using Potentiostat/Galvanostat interface 1010E (Gamry Instruments, USA) in 3.5% NaCl solution using Ag/AgCl in a saturated solution of KCl as the reference electrode. Parallel graphite rod was engaged as the counter electrode. The samples are prepared prior to Potentiodynamic testing and proper mounting is done to expose only required area. I used bottle caps for this purpose and attached copper wires behind the samples and mounted them using a room cure epoxy system as shown in Figure 23.

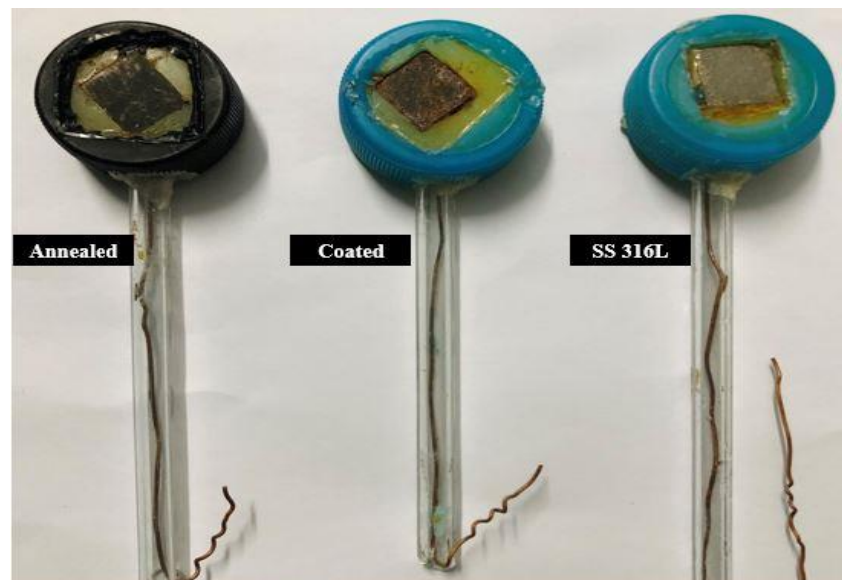


Figure 23. Samples after Potentiodynamic Testing in 3.5% NaCl solution a). Annealed b). Coated & c). SS 316L

After that testing was done one by one and the corresponding Potentiodynamic curves of bare stainless steel 316, coated substrate, and after annealing is given in the Figure 24.

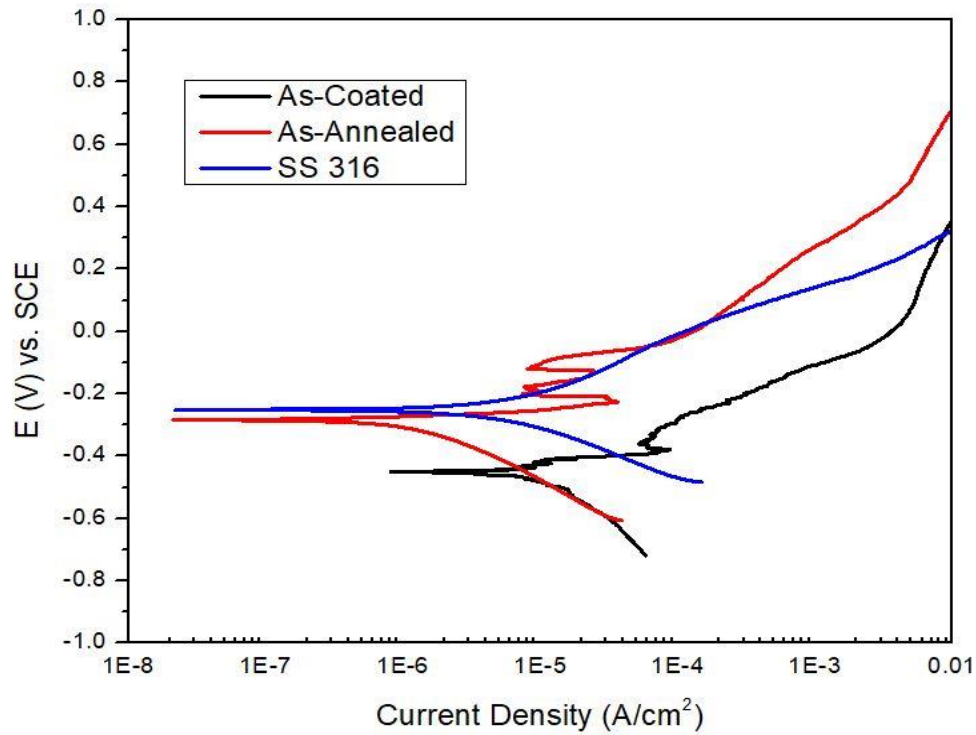


Figure 24. Curves depicting Potentiodynamic polarization/Corrosion performance of SS 316L, Coated & Annealed Sample in 3.5% NaCl

In case of stainless steel, the results revealed that the current density of $7.32 \mu\text{A}/\text{cm}^2$ which reflect that surface of bare stainless steel is affected by 3.5% NaCl solution and get corroded. The E_{corr} value was -0.245 V with anodic slop 0.215 and cathodic slope -0.167 .

In case of HEA coated stainless steel substrate, the results revealed that the current density I_{corr} was $18.31 \mu\text{A}/\text{cm}^2$ which is significantly much higher than that of the stainless steel as well as the APS sprayed annealed coating. This reflect that coating was not dense enough and it had sites exposed which were more prone to the chlorides attack on the surface. The value of current density wasn't reduced by the prepared coating, as HEA wasn't formed well enough at this stage and elements were present in the coatings thus showing lowest corrosion resistance and highest value of current

density. The corresponding values of E_{corr} was -0.454 V with anodic and cathodic slope values 0.072 and -0.169 respectively.

In case of annealed coating, the large passive region and lower values of I_{Corr} results revealed that the current density was $1.99 \mu\text{A}/\text{cm}^2$ which is significantly less than that bare stainless steel 316L and HEA coating by APS on it. From this we deduce that after annealing the coatings the microstructure was changed and all the active sites which were prone to corrosion were covered by annealing of the samples. A passive film was formed on surface of coating which decreased the current density. This phenomenon increased its corrosion performance as compared to bare substrate as well as sample in as-coated condition. The corresponding value of E_{corr} was -0.281 with anodic and cathodic slope 0.052 and -0.232 respectively. All the electrochemical values are shown in Table 5 below.

Table 5. Electrochemical data of Stainless Steel 316L, Coated Sample and Annealed Sample acquired after Corrosion Behaviour Testing in 3.5% NaCl solution

Sample	E_{corr} (mV_{SCE})	Ba (V) Anodic slope	Bc(V) Cathodic slope	I_{Corr} ($\mu\text{A}/\text{cm}^2$)	Corrosion Rate CR (mpy)
SS 316L	-0.245	0.215	-0.167	7.32	3.04
As-Coated	-0.454	0.047	-0.271	18.31	7.60
Annealed	-0.281	0.052	-0.232	1.99	0.83

Chapter 6

Conclusion and Future Work

This section confers the findings of the respective thesis and suggested future work related to the current work and is given below:-

6.1 Conclusion

NiCoCrAlFe HEA coatings were manufactured using atmospheric plasma spraying and tested for isothermal oxidation in air at 1000°C for various time durations as well as tested for corrosion performance and studied extensively via various electron microscopy. A multitude of phases dispersed randomly and evenly were discovered and an endeavour was made to understand the microstructure and oxidation behaviour of the manufactured coating. After complete examination and investigation of the coatings we found the following conclusions:-

- The microstructure examination reveals a lamellar structure where oxide stringers are found at few sites in the lamellar structure alternating with the High Entropy solid solution phase.
- Stand-off distance doesn't have a significant effect on the coatings microstructure unless it is increased or decreased for a considerable value. An optimized value for stand-off distance is better for achieving a dense and good quality thermal sprayed coatings.
- HEA is formed by annealing of thermal sprayed coatings due to diffusion of elements with each other to form maximum alloy fractions within the microstructure.
- Micro Vickers hardness (HV) value for the annealed coatings were found higher than the as-coated coatings which is due to the increased degree of lattice distortion and dislocation motion inhibition.
- Owing to its sluggish diffusion behaviour and likeness in elemental composition to that of conventional MCrAlY bond coats our HE alloy system i.e. NiCoCrAlFe can be used as a potential bond for high temperature applications.

- Corrosion performance of annealed coatings was found best among SS 316L substrate as well as the coatings in as-sprayed conditions due to shielding of pores, active sites which were prone to corrosion attack.
- Overall, these experiments gave us insights about the understanding of NiCoCrAlFe HEA formation and the flight of particles through a plasma stream in air to end up forming the coating.

6.2 Future Work

The synthesized HE powder was employed as Bond Coat for Thermal Barrier Coatings application for Gas Turbine Blade and power generation applications.

In future, the same material will be coated by thermal spraying for gas turbine blades.

Furthermore, NiCoCrAlFe High entropy Bond Coat will be studied as a potential bond coat material. We will further make composite bond coats containing NiCoCrAlFe (HEA) and on top of it standard NiCoCrAlY bond coat for future applications.

In future we can make these HE alloy coatings more efficient and specific for specific application by adding refractory elements and others like Hf, Y, and Mo etc.

Chapter 7

References

- [1] Yeh, J.-W., et al., *Nanostructured High-Entropy Alloys with Multiple Principal Elements: Novel Alloy Design Concepts and Outcomes* (2004) **6**(5): p. 299-303.
- [2] Cantor, B., et al., *Microstructural development in equiatomic multicomponent alloys* (2004) **375**: p. 213-218.
- [3] Meng, G.-H., et al., *Highly oxidation resistant and cost effective MCrAlY bond coats prepared by controlled atmosphere heat treatment* (2018) **347**: p. 54-65.
- [4] Abbas, M., L. Guo, and H.J.C.I. Guo, *Evaluation of stress distribution and failure mechanism in lanthanum–titanium–aluminum oxides thermal barrier coatings* (2013) **39**(5): p. 5103-5111.
- [5] Newaz, G., *Effect of Damage Processes on Spallation Life in Thermal Barrier Coatings* (2001) WAYNE STATE UNIV DETROIT MI.
- [6] Mendis, B., et al., *Microstructural observations of as-prepared and thermal cycled NiCoCrAlY bond coats* (2006) **201**(7): p. 3918-3925.
- [7] Padture, N.P., M. Gell, and E.H.J.S. Jordan, *Thermal barrier coatings for gas-turbine engine applications* (2002) **296**(5566): p. 280-284.
- [8] Löbel, M., et al. *Processing of AlCoCrFeNiTi high entropy alloy by atmospheric plasma spraying*. in *IOP Conference Series: Materials Science and Engineering* (2017) IOP Publishing.
- [9] Karaoglanli, A., et al., *Thermal Shock and Cycling Behavior of Thermal Barrier Coatings (TBCs) Used in Gas Turbines, Chapter 10* (2014).
- [10] Ghadami, F., et al., *Effect of bond coat and post-heat treatment on the adhesion of air plasma sprayed WC-Co coatings* (2015) **261**: p. 289-294.
- [11] Anupam, A., et al., *Understanding the microstructural evolution of high entropy alloy coatings manufactured by atmospheric plasma spray processing* (2020) **505**: p. 144117.
- [12] Mora-García, A.G., et al., *Microstructural analysis of Ta-containing NiCoCrAlY bond coats deposited by HVOF on different Ni-based superalloys* (2018) **354**: p. 214-225.
- [13] Zhang, K., et al., *Annealing on the structure and properties evolution of the CoCrFeNiCuAl high-entropy alloy* (2010) **502**(2): p. 295-299.

- [14] Vaidya, M., G.M. Muralikrishna, and B.S.J.J.o.M.R. Murty, *High-entropy alloys by mechanical alloying: A review* (2019) **34**(5): p. 664-686.
- [15] Zhang, B.-Y., et al., *Non-parabolic isothermal oxidation kinetics of low pressure plasma sprayed MCrAlY bond coat* (2017) **406**: p. 99-109.
- [16] Avci, A., A.A. Eker, and B. Eker, *Microstructure and Oxidation Behavior of Atmospheric Plasma-Sprayed Thermal Barrier Coatings*, in *Exergetic, Energetic and Environmental Dimensions* (2018) Elsevier. p. 793-814.
- [17] Kai, W., et al., *Air-oxidation of FeCoNiCr-based quinary high-entropy alloys at 700–900 C* (2017) **121**: p. 116-125.
- [18] Wang, H., et al., *Microstructural analysis and transport properties of thermally sprayed multiple-layer ceramic coatings* (2018) **27**(3): p. 371-378.
- [19] Di Ferdinando, M., et al., *Isothermal oxidation resistance comparison between air plasma sprayed, vacuum plasma sprayed and high velocity oxygen fuel sprayed CoNiCrAlY bond coats* (2010) **204**(15): p. 2499-2503.
- [20] Huang, P.-K. and J.-W.J.T.S.F. Yeh, *Effects of substrate temperature and post-annealing on microstructure and properties of (AlCrNbSiTiV) N coatings* (2009) **518**(1): p. 180-184.
- [21] Bai, M., et al., *Preparation of MCrAlY–Al₂O₃ composite coatings with enhanced oxidation resistance through a novel powder manufacturing process* (2019) **28**(3): p. 433-443.
- [22] Munawar, A.U., et al., *Microstructure and lifetime of EB-PVD TBCs with Hf-doped bond coat and Gd-zirconate ceramic top coat on CMSX-4 substrates* (2016) **299**: p. 104-112.
- [23] Munawar, A.U., *Lifetime investigations on novel thermal barrier coating systems for gas turbine applications* (2014).
- [24] Afrasiabi, A., et al., *A comparative study on hot corrosion resistance of three types of thermal barrier coatings: YSZ, YSZ+ Al₂O₃ and YSZ/Al₂O₃* (2008) **478**(1-2): p. 264-269.
- [25] Jadhav, M., et al., *An investigation on high entropy alloy for bond coat application in thermal barrier coating system* (2019) **783**: p. 662-673.
- [26] Zhou, Y., et al., *Solid solution alloys of Al Co Cr Fe Ni Ti x with excellent room-temperature mechanical properties* (2007) **90**(18): p. 181904.
- [27] Meghwal, A., et al., *Multiscale mechanical performance and corrosion behaviour of plasma sprayed AlCoCrFeNi high-entropy alloy coatings* (2021) **854**: p. 157140.

- [28] Wang, L., et al., *Microstructure evolution and mechanical properties of atmosphere plasma sprayed AlCoCrFeNi high-entropy alloy coatings under post-annealing* (2021) **872**: p. 159607.
- [29] Xiao, J.-K., et al., *Microstructure and wear behavior of FeCoNiCrMn high entropy alloy coating deposited by plasma spraying* (2020) **385**: p. 125430.
- [30] Fauchais, P.J.J.o.P.D.A.P., *Understanding plasma spraying* (2004) **37**(9): p. R86.
- [31] Garrido, B., et al., *Adhesion improvement and in vitro characterisation of 45S5 bioactive glass coatings obtained by atmospheric plasma spraying* (2021) **405**: p. 126560.
- [32] Srivastava, M., et al., *Synthesis and properties of high velocity oxy-fuel sprayed FeCoCrNi2Al high entropy alloy coating* (2019) **378**: p. 124950.
- [33] Richer, P., et al., *Oxidation behaviour of CoNiCrAlY bond coats produced by plasma, HVOF and cold gas dynamic spraying* (2010) **204**(24): p. 3962-3974.
- [34] Hsu, W.-L., et al., *Thermal sprayed high-entropy NiCo_{0.6}Fe_{0.2}Cr_{1.5}SiAlTi_{0.2} coating with improved mechanical properties and oxidation resistance* (2017) **89**: p. 105-110.
- [35] Karaoglanli, A.C., et al., *Comparison of tribological properties of HVOF sprayed coatings with different composition* (2017) **318**: p. 299-308.
- [36] Cheng, K.-C., et al., *Properties of atomized AlCoCrFeNi high-entropy alloy powders and their phase-adjustable coatings prepared via plasma spray process* (2019) **478**: p. 478-486.
- [37] Che, C., et al., *Effect of bond coat surface roughness on oxidation behaviour of air plasma sprayed thermal barrier coatings* (2008) **24**(4): p. 276-279.
- [38] Choi, H., et al., *Isothermal oxidation of air plasma spray NiCrAlY bond coatings* (2002) **150**(2-3): p. 297-308.
- [39] Anupam, A., et al., *First report on cold-sprayed AlCoCrFeNi high-entropy alloy and its isothermal oxidation* (2019) **34**(5): p. 796-806.
- [40] Rajput, A. and M. Srivastava, *HIGH TEMPERATURE OXIDATION BEHAVIOUR OF HVOF SPRAYED Ni-30 MULLITE COATING ON MILD STEEL* (2020).
- [41] Tian, L.-H., et al., *Microstructure and wear behavior of atmospheric plasma-sprayed AlCoCrFeNiTi high-entropy alloy coating* (2016) **25**(12): p. 5513-5521.

- [42] Li, T., et al., *Microstructure and wear behavior of FeCoCrNiMo0. 2 high entropy coatings prepared by air plasma spray and the high velocity oxy-fuel spray processes* (2017) **7**(9): p. 151.
- [43] Berndt, C.C. and R. McPherson, *Electron microscopic studies of plasma-sprayed coatings*, in *Advances in Materials Characterization II* (1985) Springer. p. 265-278.
- [44] Oatley, C.J.J.o.A.P., *The early history of the scanning electron microscope* (1982) **53**(2): p. R1-R13.
- [45] Mohammed, A. and A. Abdullah. *Scanning electron microscopy (SEM): A review*. in *Proceedings of the 2018 International Conference on Hydraulics and Pneumatics—HERVEX, Băile Govora, Romania* (2018).
- [46] Guo, J.Z., et al., *High-energy/power and low-temperature cathode for sodium-ion batteries: in situ XRD study and superior full-cell performance* (2017) **29**(33): p. 1701968.
- [47] Lin, D.-y., et al., *Influence of laser re-melting and vacuum heat treatment on plasma-sprayed FeCoCrNiAl alloy coatings* (2017) **24**(12): p. 1199-1205.
- [48] Meghwal, A., et al., *Thermal spray high-entropy alloy coatings: a review* (2020) **29**: p. 857-893.
- [49] Grewal, H., et al., *Microstructural and mechanical characterization of thermal sprayed nickel–alumina composite coatings* (2013) **216**: p. 78-92.
- [50] Baiamonte, L., et al., *Hot corrosion resistance of laser-sealed thermal-sprayed cermet coatings* (2019) **9**(6): p. 347.
- [51] Sundaresan, C., et al., *Comparative hot corrosion performance of APS and Detonation sprayed CoCrAlY, NiCoCrAlY and NiCr coatings on T91 boiler steel* (2021) **189**: p. 109556.
- [52] Javed, M., et al., *Corrosion and mechanical performance of HVOF WC-based coatings with alloyed nickel binder for use in marine hydraulic applications* (2021). **418**: p. 127239.